Duethmann, D., Bolch, T., Farinotti, D., Kriegel, D., Vorogushyn, S., Merz, B., Pieczonka, T., Jiang, T., Su, B., Güntner, A. (2015): Attribution of streamflow trends in snow and glacier melt-dominated catchments of the Tarim River, Central Asia. - *Water Resources Research*, *51*, 6, p. 4727-4750.

DOI: http://doi.org/10.1002/2014WR016716

AGU PUBLICATIONS

Water Resources Research

RESEARCH ARTICLE
10.1002/2014WR016716

Attribution of streamflow trends in snow and glacier melt-dominated catchments of the Tarim River, Central Asia

Doris Duethmann[1], Tobias Bolch[2,3], Daniel Farinotti[1,4], David Kriegel[1,5], Sergiy Vorogushyn[1], Bruno Merz[1,6], Tino Pieczonka[2], Tong Jiang[7,8], Buda Su[7,8,9], and Andreas Güntner[1]

[1]Section Hydrology, GFZ German Research Centre for Geosciences, Potsdam, Germany, [2]Institute for Cartography, Technische Universität Dresden, Dresden, Germany, [3]Department of Geography, University of Zurich, Zurich, Switzerland, [4]Now at Swiss Federal Institute for Forest, Snow and Landscape Research WSL, Birmensdorf, Switzerland, [5]Now at IBGW GmbH, Leipzig, Germany, [6]Institute of Earth and Environmental Science, University of Potsdam, Potsdam, Germany, [7]National Climate Centre, China Meteorological Administration, Beijing, China, [8]Collaborative Innovation Center on Forecast and Evaluation of Meteorological Disasters, Nanjing University of Information Science and Technology, Nanjing, China, [9]Xinjiang Institute of Ecology and Geography, Chinese Academy of Science, Urumqi, China

Key Points:
- Hydrological model explicitly considers the effect of glacier geometry changes on streamflow trend
- Multiobjective calibration using discharge and glacier mass balance criteria
- Increase of temperature and glacier melt played a larger role than previously suggested

Supporting Information:
- Supporting Information S1

Correspondence to:
D. Duethmann,
doris.duethmann@gfz-potsdam.de

Citation:
Duethmann, D., T. Bolch, D. Farinotti, D. Kriegel, S. Vorogushyn, B. Merz, T. Pieczonka, T. Jiang, B. Su, and A. Güntner (2015), Attribution of streamflow trends in snow and glacier melt-dominated catchments of the Tarim River, Central Asia, *Water Resour. Res.*, *51*, 4727–4750, doi:10.1002/2014WR016716.

Received 26 NOV 2014
Accepted 16 MAY 2015
Accepted article online 25 MAY 2015
Published online 30 JUN 2015

Abstract Observed streamflow of headwater catchments of the Tarim River (Central Asia) increased by about 30% over the period 1957–2004. This study aims at assessing to which extent these streamflow trends can be attributed to changes in air temperature or precipitation. The analysis includes a data-based approach using multiple linear regression and a simulation-based approach using a hydrological model. The hydrological model considers changes in both glacier area and surface elevation. It was calibrated using a multiobjective optimization algorithm with calibration criteria based on glacier mass balance and daily and interannual variations of discharge. The individual contributions to the overall streamflow trends from changes in glacier geometry, temperature, and precipitation were assessed using simulation experiments with a constant glacier geometry and with detrended temperature and precipitation time series. The results showed that the observed changes in streamflow were consistent with the changes in temperature and precipitation. In the Sari-Djaz catchment, increasing temperatures and related increase of glacier melt were identified as the dominant driver, while in the Kakshaal catchment, both increasing temperatures and increasing precipitation played a major role. Comparing the two approaches, an advantage of the simulation-based approach is the fact that it is based on process-based relationships implemented in the hydrological model instead of statistical links in the regression model. However, data-based approaches are less affected by model parameter and structural uncertainties and typically fast to apply. A complementary application of both approaches is recommended.

1. Introduction

In mountain regions, snow and glaciers play a crucial role in runoff formation. This makes these regions one of the most vulnerable environments to climate change, as temperature changes affect the ratio of rain versus snowfall, and snow and glacier melt [*Barnett et al.*, 2005]. This study focuses on streamflow variability in the Aksu catchment, located in the Central Tien Shan in Kyrgyzstan and the Xinjiang Uyghur Autonomous Region in China (Figure 1). The Aksu River is the most important tributary to the Tarim River, contributing about 80% of its streamflow (as calculated from average streamflow at the last gauges of the Aksu, Hotan, and Yarkand Rivers before their confluence forms the Tarim River, for the period 1964–2003). These water resources are of eminent importance for the population, industry, agriculture, and natural vegetation in the Tarim Basin, where the only significant water supply is via streams from the surrounding mountain regions [*Feng et al.*, 2001; *Leiwen et al.*, 2005; *Thevs*, 2011]. Several studies report increasing discharge of the Aksu headwater streams over the period 1957–2004 [e.g., *Zhang et al.*, 2010; *Krysanova et al.*, 2014]. While it is assumed that these increases are related to concurrent trends in temperature and precipitation [*Chen et al.*, 2009; *Xu et al.*, 2010; *Zhang et al.*, 2010; *Tao et al.*, 2011], a thorough attribution analysis is still missing.

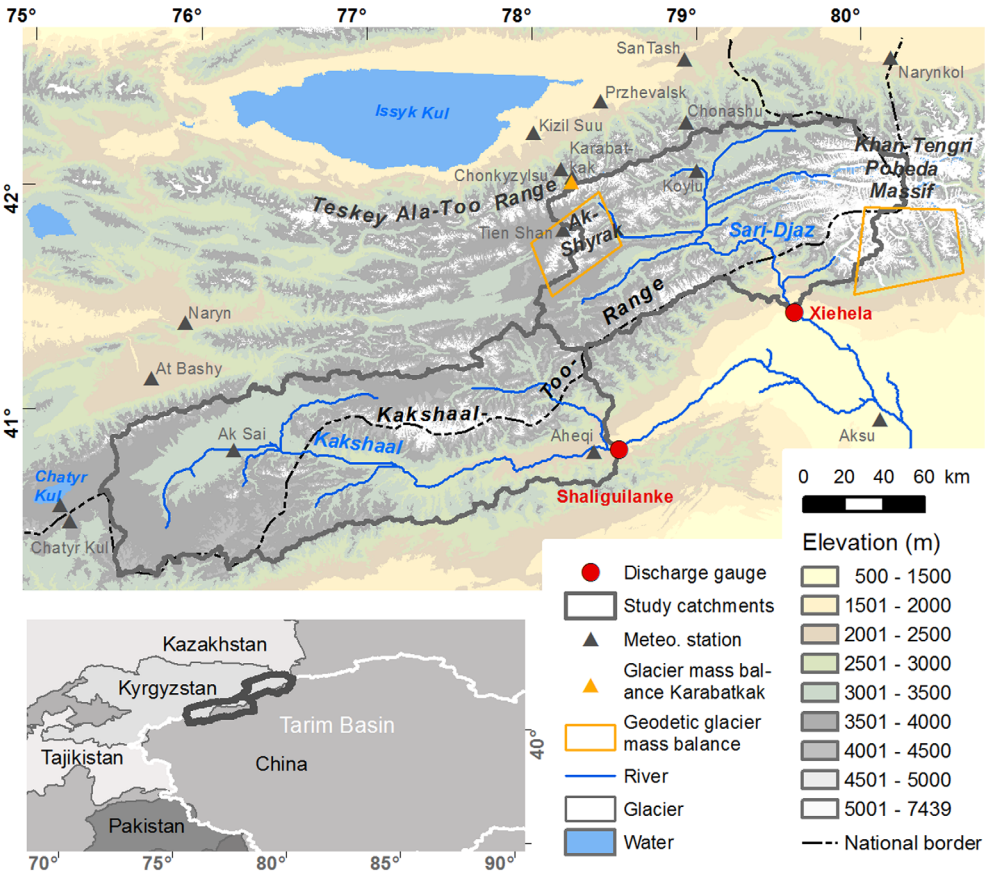

Figure 1. The study catchments, including elevation, discharge gauges, meteorological stations, and locations of Karabatkak Glacier and geodetic mass balance estimates. The inset shows the location of the study area (dark gray outline) in relation to national borders and the Tarim Basin (white outline).

The analysis of streamflow trends in mountain catchments influenced by snow and glacier melt has recently gained attention, and a number of studies (presented below) have attempted to attribute detected changes to their possible drivers. The link between trends in streamflow and possible climatic drivers may be investigated by data-based or simulation-based approaches [*Merz et al.*, 2012]. Data-based approaches directly relate changes in runoff to changes in climate without the additional step of applying a hydrological model. The analysis of concurrent trends in streamflow and climate variables can already give first insights on possible causes of detected streamflow trends [*Birsan et al.*, 2005; *Li et al.*, 2010; *Pellicciotti et al.*, 2010; *Kriegel et al.*, 2013]. The influence of glaciers on the streamflow trend can be investigated by comparative analyses of trends in glacierized and unglacierized catchments over a region for which climatic variations can be assumed similar [*Fleming and Clarke*, 2003]. For example, contrasting trends in summer discharge were observed for two catchments with differing glacier cover [*Dahlke et al.*, 2012]. For glacierized basins, the analysis of concurrent trends in temperature and precipitation can be complemented by considering glacier mass balance time series [*Li et al.*, 2010; *Pellicciotti et al.*, 2010]. Streamflow trend analyses at a high temporal resolution, e.g., using annual time series of streamflow of each day of the year, are useful to investigate temporal shifts of the streamflow regime, which may then further be related to catchment properties [*Dery et al.*, 2009; *Kormann et al.*, 2015].

Approaches based on regression analysis enable establishing a quantitative relation between trends and their possible drivers. For example, multiple linear regression was applied to investigate the role of temperature and precipitation changes for trends in fractional winter and spring runoff in mountain catchments [*Aguado et al.*, 1992; *Dettinger and Cayan*, 1995], for trends in spring snow water equivalents [*Mote*, 2006], and for streamflow and mass balance variability in glacierized catchments [*Collins*, 1987; *Moore and*

Demuth, 2001]. Generalized least squares regression allows taking care of serially correlated residuals and was for example applied to investigate whether streamflow trends are artifacts of climate variability by including climate indices in the trend analysis [*St Jacques et al*., 2010]. In glacierized catchments, increasing temperatures (without changes in precipitation) are in an initial phase expected to cause increased glacier melt discharge due to higher melt rates. However, these higher melt rates ultimately result in glacier area retreat, causing decreasing glacier melt in a later phase [*Jansson et al*., 2003; *Moore et al*., 2009; *Baraer et al*., 2012]. *Stahl and Moore* [2006] analyzed trends in the residuals of a regression model that predicted August streamflow from August temperature and precipitation and July streamflow to gain insights into whether glaciers in their study region have already passed the initial phase of increasing discharge.

Trend attribution in mountain catchments is complex due to the fact that one has to consider the influences of variations in temperature and precipitation, in seasonal snow storage, and in glacier mass balance and area at different elevations [*Molnar et al*., 2011]. For example, concurrent trends in winter streamflow and winter temperature may be found, indicating more snowmelt events or an increasing fraction of rain as compared to snow during winter. However, winter temperatures may still be well below 0°C in the largest part of the catchment and during most of the winter so that the temperature increase is not sufficient to explain the streamflow increase. To estimate whether it is physically plausible that the temperature increase caused the streamflow increase, one would have to extrapolate the temperature to different elevations in the catchment and estimate the area where rainfall or snowmelt could have occurred. This may be easier incorporated within a hydrological modeling approach that allows testing whether the hypotheses on causes for changes are plausible and whether different types of information are consistent with each other. A further advantage of the simulation-based approach is the possibility of analyzing trends in components of the water cycle which are not or cannot be measured individually [*Hamlet et al*., 2007], such as trends in soil moisture or glacier melt.

Despite these advantages, there are only few studies using simulation-based approaches for attributing streamflow trends in snow/glacier melt-dominated catchments to their possible causes. Examples are *Hamlet et al*. [2005, 2007], who applied a hydrological model to investigate the influence of precipitation and temperature changes on changes in snow water equivalent and the timing of runoff and soil moisture recharge over the western United States, or *Engelhardt et al*. [2014], who used a glaciohydrological model to explain discharge changes between different time periods. Using global climate models runs with and without anthropogenic forcing, *Hidalgo et al*. [2009] were able to attribute shifts toward earlier streamflow timing in the western United States to anthropogenic climate change. *Zhao et al*. [2013] investigated the runoff increase in the Aksu catchment by applying the Variable Infiltration Capacity model, and they attributed the runoff increase mostly to an increase in precipitation. However, their study did not consider parameter uncertainties, and observations on mass balances were not taken into account for model calibration. In such a region with large uncertainties in the precipitation data, this can lead to wrong conclusions, as an underestimation of precipitation can be compensated in the model by an overestimation of glacier melt and vice versa [*Stahl et al*., 2008; *Schaefli and Huss*, 2011]. It is therefore necessary to include glacier mass balance estimates in the model calibration procedure [e.g., *Schaefli et al*., 2005; *Stahl et al*., 2008; *Konz and Seibert*, 2010; *Mayr et al*., 2013]. As mass balance data derived by the glaciological method are only available for few individual glaciers, geodetic glacier mass balances may be applied as an alternative [*Jost et al*., 2012].

Negative glacier mass balances over a longer period result in lowering of the glacier surface elevation and reductions of the glacier area. These changes have a feedback on the glacier mass balance itself: the reduction in glacier area in the ablation zone results in less glacier melt and thus a less negative glacier mass balance, while the lowering of the glacier elevation and the associated increase in surface temperature cause both increased glacier melt and reduced snow accumulation [*Paul*, 2010]. An analysis of these effects for glaciers in Switzerland showed that the negative effect caused by glacier surface lowering compensated on average about 50% of the positive effect due to glacier area change [*Huss et al*., 2012]. While changes in glacier geometry have been taken into account in hydrological modeling for climate impact analyses [e.g., *Stahl et al*., 2008; *Huss et al*., 2010; *Nolin et al*., 2010; *Farinotti et al*., 2012; *Jost et al*., 2012], to our knowledge they have so far not been considered for the attribution of observed discharge trends.

Table 1. Area, Glacier Coverage, Elevation Range, Mean Annual Runoff, and Mean Annual Precipitation of the Two Catchments[a]

	Area (km^2)	Glacier Coverage (1970s) (%)	Elevation (m)			Runoff (1957–2004) (mm a^{-1})	Interpolated Precip. (1957–2004) (mm a^{-1})	Precip. Estimated by Hydr. Modeling (1957–2004) (mm a^{-1})
			Min.	Max.	Mean			
Kakshaal	18,410	4.4	1900	5900	3550	151	245	386 (372–399)
Sari-Djaz	12,948	20.9	1450	7100	3700	382	333	474 (450–526)

[a]Interpolated precip. is the areal precipitation estimate from interpolation of station-based observations, as described in section 3.1. The last column shows mean areal precipitation estimated from hydrological modeling (see section 3.5.1 and 4.2.1), with the ranges over the selected model solutions in parentheses.

The presented study aims at a comprehensive trend attribution for two snow and glacier melt-dominated catchments. We revisit streamflow changes in the Aksu River and apply both a data-based approach using multiple linear regression analysis, and a simulation-based approach using hydrological modeling. Applying two approaches that involve different assumptions allows us to assess the reliability of the results. For the simulation-based approach, glacier area and elevation changes are taken into account, and the model is calibrated using criteria based on daily and interannual discharge variations, interannual variations of the simulated glacier mass balance, and the cumulative glacier mass change. In this study, we investigate (1) whether the observed discharge trends can be reproduced by the regression-based approach and by the simulation-based approach and (2) to what extent changes in temperature or in precipitation contributed to the observed streamflow increase.

2. Study Area and Observed Hydrometeorological Changes

The study area comprises two headwater catchments of the Aksu River: the Kakshaal and the Sari-Djaz catchment (Figure 1 and Table 1). The lower part of the Aksu River is not considered as it hardly contributes to runoff generation and is strongly influenced by water management [*Tang et al.*, 2007]. The Kakshaal catchment (also called Toxkan or Toshkan in China) upstream of the gauge Shaliguilanke (see Figure 1 for location) has an area of 18,410 km^2. About 4.4% were covered by glaciers in the mid-1970s. With an area of 12,950 km^2, the Sari-Djaz catchment (also called Kumarik in China) upstream of the gauge Xiehela is about one third smaller but has a higher glacierization (about 21% for the mid-1970s). Only about 5% of the glacier surface in our study area is debris covered [*Pieczonka and Bolch*, 2015]. The investigated catchments have similar mean elevations (3600–3700 m), but the elevation range is higher in the Sari-Djaz (1450–7100 m) than in the Kakshaal catchment (1900–5900 m). Due to the high mountain terrain with relatively low precipitation, land cover is dominated by grassland, barren or sparsely vegetated land, and snow and ice.

Average annual precipitation over the period 1960–1990 measured at precipitation gauges within the two catchments ranges from 190 to 320 mm a^{-1} (stations Aheqi/Ahochi and Koylu, respectively (Figure 1); values without undercatch correction), but higher values are expected at exposed mountain locations. The precipitation regime shows a strong maximum in summer, typical for the Central and Southern Tien Shan [*Aizen et al.*, 1995; *Bothe et al.*, 2012]. Average annual runoff over the period 1960–1990 was 140 and 360 mm a^{-1} for the Kakshaal and the Sari-Djaz Basin, respectively [*Wang*, 2006]. The high annual runoff compared to the annual precipitation at the stations can be explained by an underestimation of the catchment-average precipitation by the precipitation stations and by additional runoff from glacier mass loss. Maximum monthly discharge occurs in July (Kakshaal) and August (Sari-Djaz) when runoff is generated by snowmelt, glacier melt, and rainfall. High discharge peaks at the Xiehela gauge can further result from quasiperiodic outbursts of the Merzbacher Lake, which occur about once a year [*Glazirin*, 2010]. The average volume of these floods was estimated at 170 $\times$ 10^6 m^3 [*Jinshi*, 1992; *Wortmann et al.*, 2013], which corresponds to around 5% of the summer (JJA) discharge at Xiehela.

Observed changes in the hydrometeorological variables and glaciers have been described in a number of studies and are only briefly summarized here (for an overview, see *Krysanova et al.* [2014]). Over the time period 1957–2004, discharge has increased by around 30% at the gauges Shaliguilanke and Xiehela [*Xu et al.*, 2010; *Kundzewicz et al.*, 2015]. Over the same period, several studies showed a temperature and precipitation increase for stations in the Chinese part of the basin [*Xu et al.*, 2010; *Zhang et al.*, 2010; *Fan et al.*,

2011; *Tao et al*., 2011], while stations close to the basin in Kyrgyzstan showed an increase in temperature but not in precipitation [*Aizen et al*., 1997, 2006].

Glacier area in the Tien Shan decreased over the last decades, and in the Central Tien Shan, from which the Aksu headwater streams drain, glacier retreat rates were generally lower than in the outer ranges [*Narama et al*., 2010; *Sorg et al*., 2012; *Unger-Shayesteh et al*., 2013]. For the Chinese part of the Aksu Basin, *Liu et al*. [2006] reported a glacier area decrease of 3.3% for the period 1963–1999, while *Pieczonka and Bolch* [2015] found a loss of 3.6 ± 4.8% for the entire Aksu Basin between ~1975 and 2008. The area loss rate was slightly higher in the Sari-Djaz subbasin and the period 1990–2010 (3.7 ± 2.7%) [*Osmonov et al*., 2013]. For the Ak-Shirak massif, glacier area losses of 8.7% for the period 1977–2003 [*Aizen et al*., 2006], and 13.6% for the period from the mid-1970s to the mid-2000s and the part draining to the Naryn Basin [*Kriegel et al*., 2013] were reported. Geodetic mass balances available for this study covered two areas adjacent to our study area (see Figure 1 for location). For the Ak-Shirak massif for the 1977–1999 period, *Surazakov and Aizen* [2006] estimated glacier thickness changes of −15.1 ± 8.2 m, based on topographic maps and the SRTM3 DEM. Assuming an ice density of 900 kg m^{-3}, this corresponds to a mass change of −0.62 ± 0.33 m water equivalent (w.e.) a^{-1}. For a region south of Tomur Peak for the 1976–1999 period, *Pieczonka et al*. [2013] derived an average glacier mass change of −0.42 ± 0.23 m w.e. a^{-1} from differencing SRTM3 and Hexagon DEMs. A new geodetic mass balance estimate covering the entire Sari-Djaz Basin shows a glacier mass loss of −0.35 ± 0.34 m w.e. a^{-1} for the time period 1974–1999 [*Pieczonka and Bolch*, 2015]. Mass loss from Karabatkak Glacier, close to the Aksu Basin in the Teskey-Ala-Too mountain range (Figure 1), is in line with these geodetic estimates, and over the period 1977–1998, an average mass loss of −0.6 m w.e. a^{-1} was measured [*Dyurgerov and Meier*, 2005; *WGMS*, 2012].

3. Data and Methods

3.1. Streamflow and Meteorological Data

Daily discharge data for the gauges Xiehela and Shaliguilanke were available for the period 1964–1987 from the Hydrological Yearbook of the Chinese Ministry of Water Resources. Monthly discharge data were available for 1957–2004 [*Wang*, 2006]. The daily data were checked for jumps to remove possible digitization errors. In cases where monthly sums of daily data did not agree with the monthly data, more trust was given to the daily data.

Daily meteorological data with variable lengths over the study period 1957–2004 from stations within and close to the study area were obtained from the Kyrgyz Hydrometeorological Service. Daily data were available from 4 stations for temperature and 13 stations for precipitation (see Figure 1). These also included data of the station Tien Shan, which was included in the analysis despite a relocation of the station in 1998/1999 (information from the Kyrgyz Hydrometeorological Service) since visual analyses did not indicate a clear inhomogeneity (see supporting information for discussion). Further monthly station data (10 stations for temperature and 3 stations for precipitation, Figure 1) were downloaded from a collection of the Asia-CryoWeb group at the University of Idaho (http://www.asiacryoweb.org).

The temperature and precipitation station data were spatially interpolated to a 2 km × 2 km grid (see supporting information for details). A varying number of meteorological stations over time may lead to inhomogeneities of the resulting data set. However, in our study area, only two stations cover the whole period, and using only these data would likely reduce the ability of a hydrological model in representing the observed discharge. To use most of the available data but minimize the problem of possible inhomogeneities in the resulting data set, we interpolated anomalies to a monthly climatology of a reference period. Compared to direct interpolation of the data, interpolation of anomalies reduces the effect of a varying station network [*Chen et al*., 2002; *Daly*, 2006].

In addition to temperature and precipitation data, time series of humidity and radiation were required to drive the hydrological model. As hardly any measured time series were available, the 0.5° Watch Forcing Data based on ERA-40 (WFD-E40) [*Uppala et al*., 2005; *Weedon et al*., 2011] were used for the period 1957–2001. These were complemented with ERA-Interim based Watch Forcing Data (WFD-EI) [*Dee et al*., 2011; *Weedon et al*., 2014] for the period 2002–2004. Correspondence between the two data sets was ensured by multiplying the WFD-EI data with a bias factor, which was calculated for each day of the year over the common period 1979–2001 using 31 day moving averages.

3.2. Drivers Included in the Attribution

While this study focused on the influence of temperature and precipitation changes on the observed streamflow increase, rigorous trend attribution studies should also comprise a search for possible alternative drivers and evidence that these are inconsistent with the observed changes [*Merz et al*., 2012]. Such alternative drivers could be changes in other meteorological variables than temperature or precipitation, in water management, or in land cover. Measured time series for radiation, wind speed, or humidity were not available. Data for these variables were only available from reanalysis data, which, due to changes of the observing system over time, are less suited for trend analyses [*Bengtsson et al*., 2004]. Reanalysis data for these variables were therefore not interpreted for trend attribution; however, they had to be applied as input for the hydrological model. Based on statements from local water authorities, visual analysis and double mass testing of the streamflow time series, and the fact that the catchments are hardly populated and that agricultural land use is negligible, changes in water management were excluded. Land cover changes in the upstream parts of the Aksu between the 1970s and 2008 were a decrease in glacier area and an increase in grassland [*Zhou et al*., 2010]. While their study showed a strong increase of cropland in the downstream part of the Aksu basin, this was not the case in the upstream part considered in our study. The effect of changes in glacier area and glacier surface elevation is explicitly considered in our study with the simulation-based approach.

3.3. Trend Analysis

Throughout this paper, trends were estimated using Sen's slope estimator [*Sen*, 1968]. This estimator is less affected by outliers and nonnormally distributed data than linear regression [e.g., *Yue et al*., 2003]. Trend significance was assessed using the nonparametric Mann-Kendall test [*Mann*, 1945; *Kendall*, 1975], which is robust against outliers and also suited for nonnormally distributed data or data with nonlinear trends. Since serial correlation may lead to an overestimation of the trend, we applied so-called trend free prewhitening (TFPW), thus removing the influence of a lag-one autoregressive process [*Yue et al*., 2002]. In contrast to the direct application of prewhitening to the original time series, TFPW preserves the trend magnitude. Test results are reported as *p*-values, i.e., the probability of being wrong if rejecting the null hypothesis of no trend.

3.4. Data-Based Attribution Analysis

Multiple linear regression analysis was conducted to estimate the influence of temperature and/or precipitation variations on interannual streamflow variations. This analysis was performed at a seasonal time scale to consider possibly varying influences in the different seasons (DJF, MAM, JJA, and SON). The dependent variable was represented by annual series of spring (summer, autumn, and winter) runoff. Possible predictors included:

1. Temperature (T) and precipitation (P) of the current season,
2. Precipitation accumulated over 1–3, 1–6, 1–9, 1–12, and 13–24 months before the current season (P_{1-3}, P_{1-6}, P_{1-9}, P_{1-12}, P_{13-24}),
3. Temperature of the last summer, defined as average temperature over JJA, MJJA, JJAS, and MJJAS (T_{JJA}, T_{MJJA}, T_{JJAS}, and T_{MJJAS}), and of the summer before last summer (T_{JJA-1}).

Temperature and precipitation aggregated over periods before the current season were included to represent release from catchment storage (including snow storage). For temperature from previous seasons, we focused on summer temperatures, since these are expected to have a strong influence on discharge through their control on glacier melt. While we tested the use of T_{JJA}, T_{MJJA}, T_{JJAS}, and T_{MJJAS} as possible predictors, they were not allowed to be simultaneously included in one regression model. Multiple linear regression was performed for all combinations of the explanatory variables (2048 combinations), i.e., best subset selection. Models were selected based on the Bayesian information criterion (BIC) [*Schwarz*, 1978]. Models with a high level of multicollinearity, i.e., with variance inflation factors (VIFs) >10, were not considered [*Draper and Smith*, 1998]. It was further analyzed whether including interaction terms of the variables included in the first step led to improved models. The regression residuals were analyzed for normality and autocorrelation. Normality was checked using normal-probability plots, complemented with formal testing using the Lilliefors test [*Lilliefors*, 1967]. Autocorrelation was checked by inspecting the autocorrelation function, complemented with formal testing using the Ljung-Box Q test [*Ljung and Box*, 1978]. For models with

nonnormally distributed residuals, it was checked whether performing the regression with log-transformed discharge led to better results. The residuals were analyzed for trends, which can indicate nonstationarity. For example, the effect of temperature variations may vary over time due to changes in the glacier geometry [*Stahl and Moore*, 2006].

The influence of changes in temperature and precipitation on the discharge trend was investigated by applying the regression model with detrended temperature and precipitation time series as input. For this purpose, temperature or precipitation time series that contained no changes over time (i.e., no trends nor changes of the daily or interannual variability) were generated by applying the same 1 year daily time series to all years in the simulation period. The daily time series of an arbitrary year in the middle of the study period was selected (the year 1980 was used), and a linear scaling was applied to the daily values so that the monthly means corresponded to the climatological means of the study period 1957–2004.

3.5. Simulation-Based Analysis

3.5.1. WASA Hydrological Model

The hydrological model WASA (Model of Water Availability in Semi-Arid Environments) [*Güntner*, 2002; *Güntner and Bronstert*, 2004] is a semidistributed model with conceptual and process-orientated approaches. The model has been adapted for applications in mountain regions with previous applications in Central Asia [*Duethmann et al*., 2013, 2014]. The original spatial discretization based on hillslopes [*Güntner and Bronstert*, 2004; *Francke et al*., 2008] was modified into an approach based on hydrological response units (HRUs) as it allows faster computations. The model has routines for snow versus rain differentiation, snow and glacier melt, glacier mass balance, interception, evapotranspiration, infiltration and saturation excess runoff, interflow, and groundwater runoff. The snow and glacier modules are outlined below and a more detailed description including model equations can be found in the supporting information.

If the air temperature falls below a calibrated threshold, precipitation is considered as snow. The spatial variability of snow within an HRU is represented using a snow depletion curve [*Liston*, 2004]. Snowmelt is calculated with a temperature-index approach [*Hock*, 2003], where the melt factor varies in a sinusoidal form between a minimum value at the winter solstice and a maximum value at the summer solstice, reflecting the increase in incoming solar radiation [*Anderson*, 1973]. Glacier melt is simulated using the same approach as for snowmelt but with a different melt factor. The glacier mass balance is calculated from snowfall onto the glacier, minus glacier- and snowmelt from the glacier area. The effect of debris cover is implicitly accounted for in our results, as model parameters are calibrated against geodetic glacier mass balances, which include both glaciers with and without debris cover (see supporting information).

The model has 13 calibration parameters (supporting information Table A1). Due to the large uncertainties in areal precipitation, the calibrated parameters include a precipitation bias factor. In mountain areas, estimating areal precipitation from sparsely distributed precipitation stations results in high uncertainties. In such cases, hydrological modeling or mass balance modeling in combination with observed discharge and glacier volume changes can be a good alternative for evaluating and correcting areal precipitation estimates [*Duethmann et al*., 2013; *Immerzeel et al*., 2015]. The precipitation bias factor is applied as a constant factor to the precipitation input, e.g., a precipitation bias factor of 1.5 means that precipitation used in the model is 50% higher than the original precipitation input. The bounds for the calibration parameters were set according to *Duethmann et al*. [2014], but with larger ranges for the groundwater delay factor (200–1000 days) and the precipitation bias factor (0.5–2.5).

3.5.2. Model Setup

The WASA model was set up using the data sources listed in Table 2. The two study catchments were subdivided into 16 and 13 subcatchments with an average size of 1100 km^2. Within each subcatchment, HRUs were defined as 200 m elevation bands, since differences in elevation rather than differences in land cover or soil (which are furthermore in mountain regions often related to elevation) were assumed most important for differences in hydrological processes. This resulted in 202 (Kakshaal) and 219 (Sari-Djaz) HRUs. Each HRU was assigned its glacier fraction (based on the 1970s glacier inventory) [cf., *Pieczonka and Bolch*, 2015], dominant land cover, and dominant soil. All meteorological data were spatially averaged to the level of subcatchments. Temperature data were scaled to the average elevation of a HRU using the estimated lapse rates.

Table 2. Spatial Data Sets Used for Setting Up the WASA Model

Data Type	Data Source	Resolution	Reference
DEM	SRTM DEM	90 m	*Jarvis et al.* [2008]
Glacier outlines 1970s	Delineated from: KH-9 Hexagon images and Landsat MSS images (1970s)	7.6 and 79 m	*Pieczonka and Bolch* [2015]
Glacier outlines ~2008	Delineated from: Landsat TM and Landsat ETM+ images (2007–2010)	30 m	*Osmonov et al.* [2013] and *Pieczonka and Bolch* [2015]
Soil types	Harmonized World Soils Database	1:1,000,000	*FAO/IIASA/ISRIC/ISS-CAS/JRC* [2012]
Land cover	MODIS land cover product MOD12Q1 collection 5.1	1:1,000,000	*Friedl et al.* [2002]

3.5.3. Changes in Glacier Area and Elevation

Over the 48 year study period, effects of changes in glacier area and glacier surface elevation cannot be neglected. Glacier area changes were derived from two glacier inventories to ensure a close representation of the observed changes in the model. Glacier inventories were available for ~1975 and for ~2008 (see Table 2) [*Osmonov et al.*, 2013; *Pieczonka and Bolch*, 2015]. Based on the two glacier inventories, linear decrease rates in area were assumed for each individual glacier. Glacier areas in the model were then updated annually according to these decrease rates during the period 1975–2004. Glacier outlines for the beginning of our study period were not available. For the period before 1975, unchanged glacier outlines were assumed. This was regarded a more plausible assumption than extending the linear trend backwards in time, as observed glacier area changes in the Ak-Shirak massif for 1943–1977 were considerably smaller than for 1977–2003 [*Aizen et al.*, 2006]. Furthermore, observed glacier mass balances in Central Asia were not far from balance in the 1960s and started to become predominantly negative in the mid-1970s [*Sorg et al.*, 2012; *Unger-Shayesteh et al.*, 2013].

In order to account for glacier elevation changes the Δh-approach by *Huss et al.* [2010] was applied (see supporting information for details). The calculation of glacier thickness changes is performed on an annual basis individually for each glacier. Glaciers were subdivided into 50 m elevation bands for this purpose. Glacier elevation changes were restricted by glacier thickness, i.e., no further reduction in glacier elevation was allowed if the accumulated elevation change exceeded the estimated glacier thickness. The glacier ice thickness distribution of each individual glacier was estimated based on the Glabtop2 model introduced by *Linsbauer et al.* [2012] and modified by *Frey et al.* [2014] using the filled SRTM DEM and the 1970s glacier inventory as input.

3.5.4. Multiobjective Model Calibration

3.5.4.1. Calibration Criteria for Discharge

Two criteria (f_{Q_1} and f_{Q_2}, equation (1) and (4)) were used for the calibration to discharge. f_{Q_1} (equation (1)) was applied to ensure a good model performance with respect to the observed hydrograph. In order to achieve a good performance both in high and low flow periods, we used a balanced Nash-Sutcliffe criterion for daily discharge values, which was defined as average of E_d (equation (2)) and E_d^{log} (equation (3))

$$f_{Q_1} = 0.5 \cdot \left(E_d + E_d^{log}\right), \tag{1}$$

with

$$E_d = 1 - \frac{\sum_{t=1}^{T}\left(Q_{obs}(t) - Q_{sim}(t)\right)^2}{\sum_{t=1}^{T}\left(Q_{obs}(t) - \overline{Q_{obs}}\right)^2}, \tag{2}$$

$$E_d^{log} = 1 - \frac{\sum_{t=1}^{T}\left(log(Q_{obs}(t)) - log(Q_{sim}(t))\right)^2}{\sum_{t=1}^{T}\left(log(Q_{obs}(t)) - \overline{log(Q_{obs})}\right)^2}. \tag{3}$$

$Q_{obs}(t)$ and $Q_{sim}(t)$ are the observed and simulated discharge at time t, respectively, and T is the number of time steps.

Since f_{Q_1} is not very sensitive to interannual discharge variations, a criterion based on annual time series of seasonal discharge was formulated additionally

$$f_{Q_2} = E^{bal}_{DJF} + E^{bal}_{MAM} + E^{bal}_{JJA} + E^{bal}_{SON}, \quad (4)$$

where E^{bal}_{DJF} (E^{bal}_{MAM}, E^{bal}_{JJA}, E^{bal}_{SON}) is the balanced Nash-Sutcliffe criterion (cf. equation (1)) calculated from annual series of observed and simulated discharge for the winter (spring, summer, and autumn) season.

3.5.4.2. Calibration Criteria for Glacier Mass Balance

We also applied two criteria for the calibration against glacier mass balances using a time series of observed glacier mass balances for Karabatkak Glacier (see Figure 1 for location) for the period 1957–1998, and geodetic mass balances for two areas adjacent to our study area (see section 2). The correlation between the simulated catchment-average mass balance and the glacier mass balance time series of Karabatkak was used as a criterion reflecting the year-to-year variation of the glacier mass balance (f_{gl_1}). The geodetic estimates, which are representative for a larger area but only give one estimate over the 1976–1999 period, were applied as criterion for the cumulative mass change (f_{gl_2}). Using the mean of the two geodetic estimates and the larger of the two uncertainty ranges, the criterion f_{gl_2} was formulated as a triangular fuzzy membership function with a value of 1 if the simulated mass balance over 1976–1999 matches the mean value of -0.52 m w.e. a^{-1}, a value of 0 if the simulated mass balance was outside the estimated uncertainty range of -0.85 to -0.19 m w.e. a^{-1}, and linearly increasing/decreasing values in between.

3.5.4.3. Optimization Algorithm

In the context of multiobjective optimization, we seek a set of Pareto optimal (or nondominated) solutions instead of a single optimum solution. For each of the solutions belonging to this Pareto optimal set, none of the objective functions can be improved without degradation in at least one of the other objective functions. In this study, the location of the Pareto optimal set was estimated using the Epsilon-Dominance Nondominated Sorted Genetic Algorithm II (ε-NSGAII) [*Kollat and Reed*, 2006], which proved to be efficient and effective in studies comparing different multiobjective optimization algorithms [*Kollat and Reed*, 2006; *Tang et al.*, 2006]. The density of the final nondominated solutions is controlled using the concept of ε-dominance. For each objective function, the user defines an ε-value, which is the smallest difference in the function that is considered relevant. For this study, the initial population size was set to 32, the maximum run time to 30,000 simulations, and ε-values were set to 0.01 for all four objectives as the different objectives vary in the same order of magnitude. Other algorithm parameters were adopted from *Kollat and Reed* [2006].

The model was calibrated for the period 1976–1999, according to the available geodetic glacier mass balance estimates. A 2 year period prior to the calibration period was used for model initialization. Due to missing daily runoff data after 1987, f_{Q_1} only refers to the period 1976–1987. The remaining part of the available time series from 1957 to 1975 and 2000 to 2004 was used as validation period.

3.5.4.4. Selection of Solutions for Further Evaluation

After model calibration, solutions were selected from the Pareto optimal set for further evaluation. Solutions with a glacier mass balance outside the uncertainty ranges of the geodetic estimate ($f_{gl_2} = 0$), or low performance with respect to daily or interannual variations of discharge were excluded. After inspecting the achieved solutions, the threshold for exclusion with respect to interannual variations of discharge was set to $f_{Q_2} < -2$. As the remaining solutions all showed a good performance with respect to daily discharge ($f_{Q_1} > 0.75$), no additional threshold was set for f_{Q_1}. Since the model was applied to analyze causes for changes in discharge, the ability of the model to represent observed discharge trends was set as a further criterion. For this purpose, trends in seasonal discharge time series were calculated over the whole study period, as the calibration or validation periods were regarded as too short for the calculation of trends. Solutions which did not simulate a significant positive (negative) trend ($p > 0.1$), even though the observed time series showed a positive (negative) trend, were excluded from further evaluation.

3.5.5. Simulation-Based Attribution

For the simulation-based approach, attribution was performed in two steps. The direct effects of precipitation and temperature changes were assessed using simulation experiments with a constant glacier geometry and detrended temperature and precipitation time series. The effect of the precipitation and temperature changes is further modified through changes in glacier geometry. This was evaluated using simulations with the original temperature and precipitation time series by comparing simulations with and without considering changes in glacier geometry. Changes in glacier geometry are a response to climatic

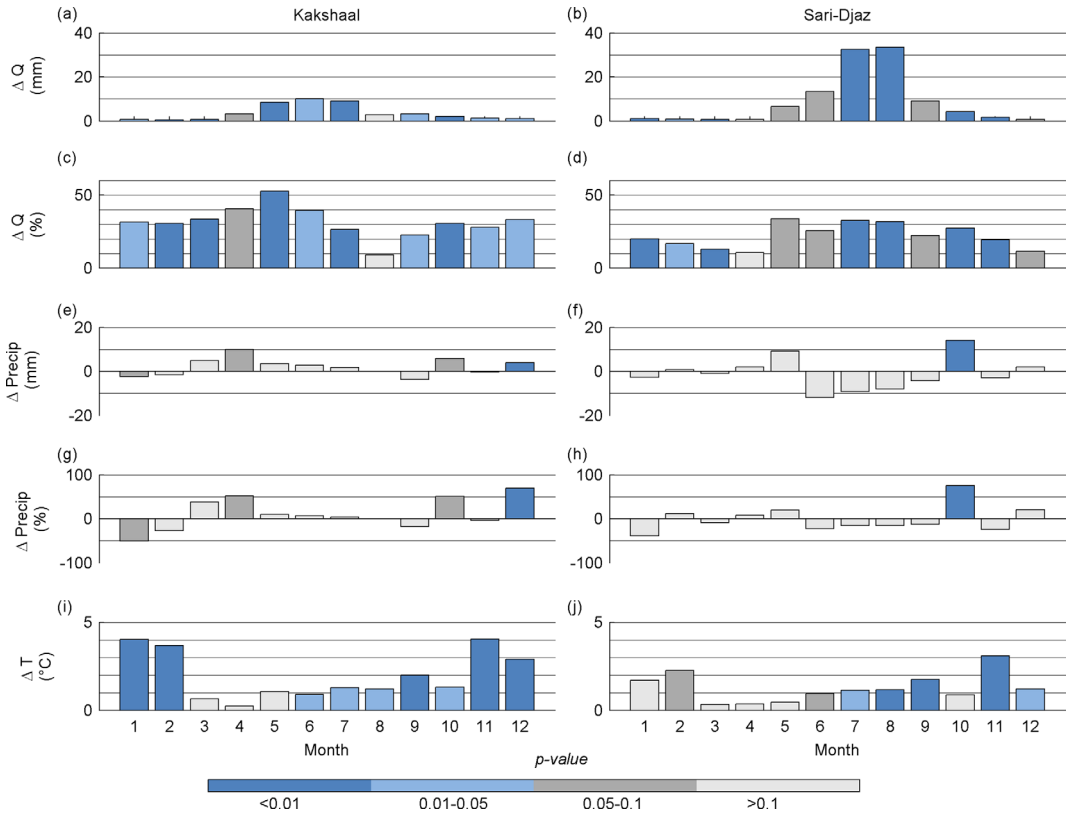

Figure 2. Monthly changes (a–d) in discharge, (e–h) in catchment-average precipitation, and (i–j) in temperature for the period 1957–2004 for the Kakshaal and the Sari-Djaz catchment. Changes in discharge and precipitation are reported in absolute (mm) and relative values (%). Bar colors indicate the significance level of the Mann-Kendall trend test.

variations, and both effects are thus closely intertwined. To estimate the overall effect of temperature and precipitation changes on the streamflow trend, changes in glacier geometry were tentatively assumed largely a response to temperature and precipitation changes during the study period, neglecting glacier surges or delayed responses to past changes.

4. Results

4.1. Data-Based Analysis

4.1.1. Trend Analysis of Discharge, Precipitation, and Temperature

In both catchments the trend analysis revealed increasing discharge in all months over the period 1957–2004 (Figures 2a–2d), in agreement with previous studies [e.g., *Xu et al*., 2010; *Kundzewicz et al*., 2015]. For the Kakshaal catchment, trends were significant at the 5% level in nearly all months. The highest absolute increases in monthly discharge occurred during May–July. In most months, discharge increased by around 30% (relative changes with respect to the mean of the study period), with larger changes in May and lower changes in August. In the Sari-Djaz catchment, the largest absolute increases in discharge were observed for July and August, where monthly discharge increased by 33 mm, or 32%.

Changes in precipitation show a less clear picture, with both increases and decreases (mostly not significant), (Figures 2e–2h). The summer months, which are the months with the highest precipitation, only show insignificant changes in both catchments.

Temperature, in contrast, increased during all months in both catchments (Figures 2i and 2j). In the Kakshaal catchment, temperatures increased most strongly during the winter months, with changes of 3–4 K over the 48 year study period. In the Sari-Djaz catchment, significant trends ($p \leq 0.05$) occurred mostly during the second half of the year from July to December. Relatively large positive trends but with slightly lower significance levels occurred in January and February.

Table 3. Results of the Linear Regression Analysis of Discharge: Coefficient of Determination (R^2), Trend in Observed Discharge (Q_{obs}), and Trend in Discharge of the Regression Model (Q_{regr}) With Original Precipitation and Temperature Input, Original Precipitation and Detrended Temperature Input, and Detrended Precipitation and Original Temperature Input and Corresponding *p*-Values, As Well As the Variables Included in the Regression Models With Their Standardized Coefficients

		Q_{obs}		Q_{regr}: Original P, Original T		Q_{regr}: Original P, Detrended T		Q_{regr}: Detrended P, Original T		Included Variables	
	R^2	Trend (mm)	*p*-Value	Trend (mm)	*p*-Value	Trend (mm)	*p*-Value	Trend (mm)	*p*-Value	Variable	Standardized Coefficient
Kakshaal											
Winter	0.67	2.5	<0.01	2.3	<0.01	1.1	0.32	1.6	<0.01	P_{13-24}	0.25
										P_{1-6}	0.78
										T_{JJAS}	0.51
Spring	0.33	14.1	<0.01	7.3	<0.01	2.6	0.35	7.0	0.01	T_{JJA}	0.53
										P_{1-9}	0.60
Summer	0.54	27.4	<0.01	24.3	<0.01	17.6	0.07	10.1	0.01	T	0.38
										P	0.53
										P_{1-9}	0.48
Autumn	0.48	6.1	0.02	7.2	0.01	2.1	0.35	5.7	<0.01	T	0.37
										P	0.39
										P_{1-3}	0.33
Sari-Djaz											
Winter	0.49	3.0	<0.01	2.1	0.01	0.2	0.80	1.1	0.01	T	−0.26
										P_{1-3}	0.46
										T_{JJAS}	0.51
Spring	0.11	7.8	0.01	1.5	0.83	0.0	0.92	1.1	0.82	T	0.33
Summer	0.67	76	<0.01	71	<0.01	2.2	0.72	71.7	<0.01	T	0.67
										P_{13-24}	−0.13
										T_{MJJAS}	0.32
Autumn	0.30	11.9	0.09	13.6	<0.01	0.0	0.76	13.1	<0.01	T	0.55

4.1.2. Multiple Linear Regression

4.1.2.1. General Model Performance and Included Variables

The regression model generally resulted in coefficients of determination (R^2) between 0.3 and 0.7 (Table 3 and Figure 3); however, the model fit was only poor for spring in the Sari-Djaz catchment ($R^2 = 0.1$).

For the Kakshaal catchment, variables for precipitation and temperature were included in all seasons, with a stronger influence of precipitation (as shown by the standardized coefficients, Table 3). For the summer and autumn seasons, variables included in the regression were temperature and precipitation of the current season and a measure for accumulated precipitation over previous months. For winter and spring, variables for accumulated antecedent precipitation and temperature of last summer were included. Winter discharge was also influenced by long-term storage effects, represented by precipitation of the year before last year. For the Sari-Djaz catchment, generally variables based on temperature were selected. The lower influence of precipitation is related to a higher contribution of glacier melt as compared to the Kakshaal catchment [*Krysanova et al.*, 2014]. The negative coefficients for temperature in the model for winter and for last year's precipitation in the model for summer are difficult to explain. While the standardized coefficients for these variables only show a small influence compared to the other included predictors, these models should be considered with care. Interaction terms were not included in any of the models; in two cases where including an interaction term led to improved BIC values these models were rejected due to VIFs >10. Trends of discharge from the regression models were generally slightly lower than trends of the observed discharge, except for autumn (Table 3).

4.1.2.2. Analysis of Residuals

Plots of the residuals against the included predictors did not indicate that the assumed linear relationships should be replaced by nonlinear ones. For most models, the residuals appear to be uncorrelated and normally distributed. Deviations from a normal distribution occurred in the models for spring and summer for the Sari-Djaz catchment. For the latter, normally distributed residuals were achieved by choosing the second best model according to BIC. For the model for spring for the Sari-Djaz catchment, using log-transformed discharge values reduced the deviations of the residuals from a normal distribution. However, the linear model was kept because the model based on log-transformed discharge still performed poorly in

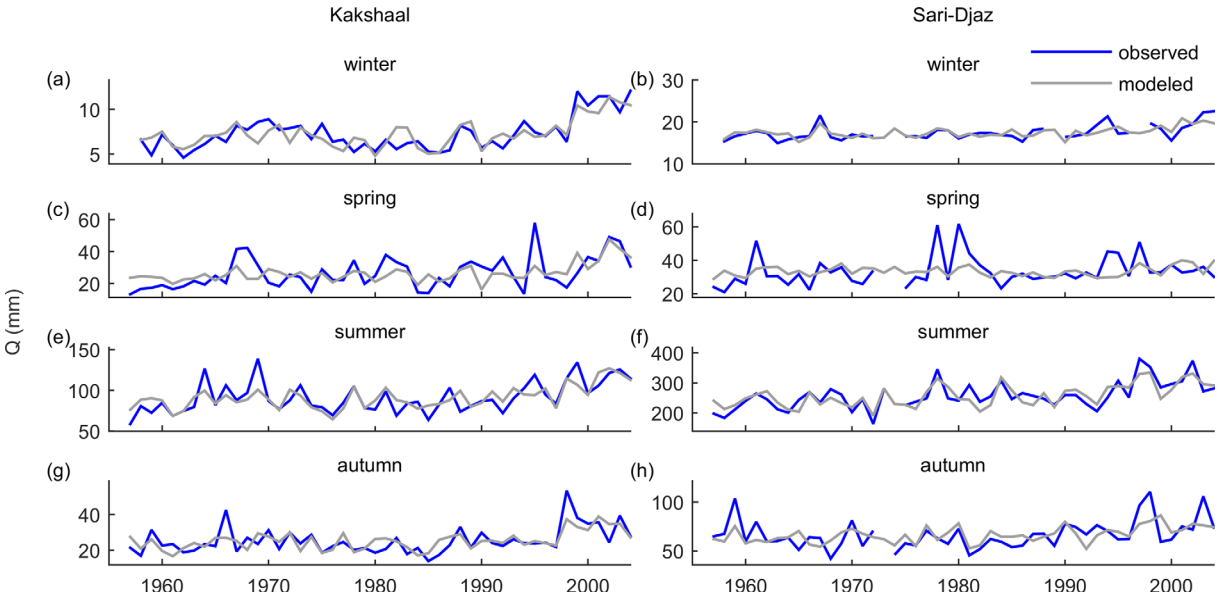

Figure 3. Annual time series of seasonal discharge from observations and the regression model for the Kakshaal and the Sari-Djaz catchment.

terms of R^2 and its ability to represent the observed trend. None of the models revealed a temporal trend in the residuals.

4.1.2.3. Influence of Temperature and Precipitation Changes on Discharge Trends

Application of the regression models with detrended temperature and precipitation time series indicates that streamflow increases in the Kakshaal catchment were caused by increases in temperature and in precipitation (Table 3 and Figure 9). In contrast, streamflow trends in the Sari-Djaz catchment were dominantly attributed to increases in temperature, and precipitation changes only played a marginal role (Table 3 and Figure 9).

4.2. Simulation-Based Analysis

4.2.1. General Model Performance

While there were no clear trade-offs between the two objective functions for discharge (f_{Q_1} and f_{Q_2}), trade-offs were apparent between the discharge and glacier objective functions, and to a very small extent between the two glacier objective functions (Figure 4). A distinct trade-off is observed between f_{Q_1} and f_{gl_1}, and this trade-off was larger for the Sari-Djaz than for the Kakshaal catchment. From the resulting Pareto set, solutions were selected for further evaluations if they showed an acceptable performance in terms of interannual discharge variation, if the simulated glacier mass balance was inside the range given by the geodetic estimate, and if a significant trend for seasonal streamflow was simulated when the observed time series displayed a trend (see section 3.5.4.4), resulting in the selection of 28 solutions for the Kakshaal and 6 solutions for the Sari-Djaz catchment.

Daily and monthly discharge variations are well represented by the model (Table 4 and Figures 5 and 6). The slightly lower model performance in the Kakshaal catchment is likely related to the stronger influence of precipitation in this catchment, which is generally associated with higher uncertainties than temperature. Large deviations for some flood peaks at the Sari-Djaz gauge (Figure 6) can be related to GLOFs from Merzbacher Lake [*Glazirin*, 2010; *Krysanova et al*., 2014], which cannot be simulated by the WASA model.

The dynamics of the simulated catchment-average glacier mass balance is generally similar to the observed mass balance of the Karabatkak Glacier (Figure 7). The low correlation value between the time series at Karabatkak and the simulated glacier mass balance in the Sari-Djaz Basin (Figures 4 and 7) results largely from an underestimation during the last 5 years. For the period 1976–1999, for which geodetic glacier mass balances were available, the mass balance was simulated to be between −0.85 and −0.25 m w.e. a^{-1} (Kakshaal catchment), and between −0.83 and −0.51 m w.e. a^{-1} (Sari-Djaz catchment). Over the complete

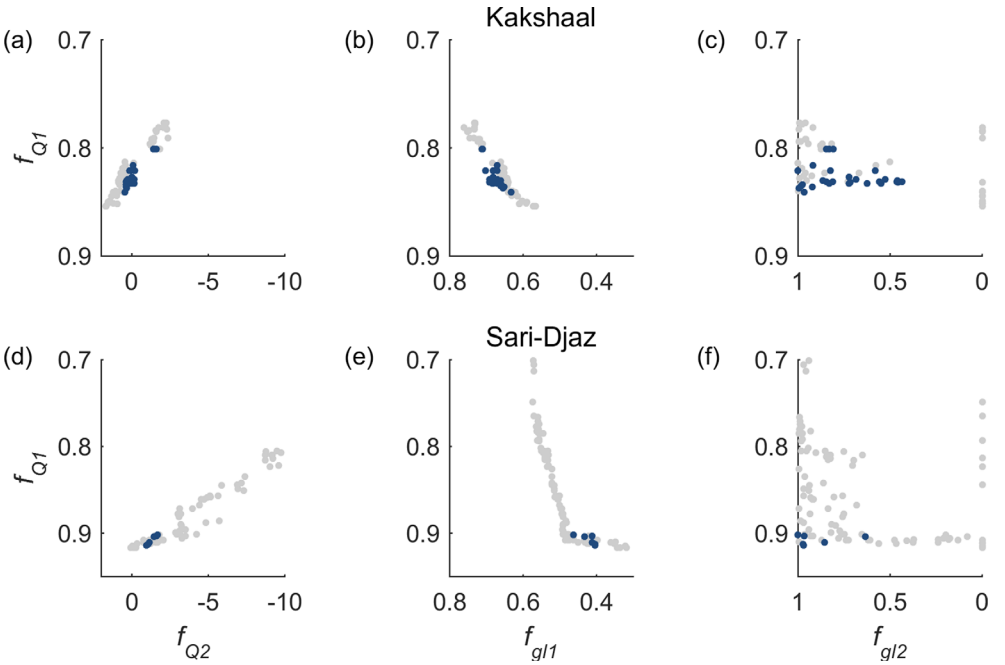

Figure 4. Trade-off curves of model performance with respect to daily discharge (f_{Q_1}) against model performance with respect to interannual discharge variations (f_{Q_2}), glacier mass balance time series at Karabatkak Glacier (f_{gl_1}), and the geodetic glacier mass balance (f_{gl_2}) for the two study catchments. Axes are plotted in reverse order so that optimum solutions always plot in the lower left corner. Blue dots show solutions used for further analyses, gray dots show solutions which were excluded due to too low performance with respect to f_{Q_2}, f_{gl_2}, or representation of observed trends (see section 3.5.4.4).

simulation period 1957–2004, the simulated mass balance was estimated between −0.76 and −0.13 m w.e. a^{-1} for the Kakshaal and between −0.77 and −0.40 m w.e. a^{-1} for the Sari-Djaz catchment.

The simulated fraction of runoff from glacier melt, defined as melt water from glacier ice/firn, without snowmelt or rain from glacier areas, may be approximated as the simulated glacier melt divided by the simulated runoff, assuming that evaporation from glacier melt is small. This results in glacier melt contributions to runoff of 9–24% for the Kakshaal catchment, and 35–48% for the Sari-Djaz catchment (uncertainty range results from parameter uncertainties). The glacier imbalance contribution to runoff is only slightly lower with 4–21% for the Kakshaal catchment and 21–40% for the Sari-Djaz catchment.

The calibrated precipitation bias factor (see section 3.5.1) allowed us to estimate the areal precipitation. The catchment-average precipitation was estimated about 50% higher than the original estimates based on interpolated precipitation data (Table 1). It reached values of about 370–400 mm a^{-1} for the Kakshaal and 450–530 mm a^{-1} for the Sari-Djaz catchment.

4.2.2. Model Performance With Respect to Interannual Variability of Discharge

While the model performance is high for daily or monthly time series, it is considerably lower when looking at interannual variations of annual or seasonal flow. This is because seasonal variations between winter low flow and summer high flow are much more distinct than interannual variations. For the Kakshaal catchment, R^2 values between simulated and observed series of average annual flow over the whole study period are between 0.61 and 0.64 (Table 5). Comparable fits were also achieved for annual series of seasonal flow, except for spring where discharge and its interannual variation are underestimated by the model. The simulated streamflow follows the long-term variations in observed discharge over the 48 year period with low discharge values at the beginning of the time period and around 1980, and higher discharge in the late 1960s and particularly after 1995 (Figure 8a). In the Sari-Djaz catchment, model performance for interannual variation of annual or seasonal values is lower than for the Kakshaal catchment (Table 5). This is mostly due to larger deviations during the last ∼10 years (Figure 8), and generally low performance in winter and spring. A reason for the larger deviations of the hydrological model for the last ∼10 years could be the lower availability of precipitation data during that period. In both catchments, the observed runoff shows

Table 4. Range of Nash-Sutcliffe Efficiency (E_d), Nash-Sutcliffe Efficiency Calculated for Logarithmic Discharge Values (E_d^{log}), and Volume Bias for Daily and Monthly Discharge During the Calibration and Validation Period for the Selected Parameterizations of the WASA Model

	E_d		E_d^{log}		Volume Bias (%)	
	Kakshaal	Sari-Djaz	Kakshaal	Sari-Djaz	Kakshaal	Sari-Djaz
Daily						
Calibration	0.77–0.82	0.85–0.87	0.84–0.87	0.95–0.96	−5 to 8	1–9
Validation	0.67–0.73	0.80–0.84	0.82–0.86	0.94–0.95	−7 to 8	7–14
Monthly						
Calibration	0.81–0.86	0.91–0.94	0.88–0.91	0.96–0.96	−6 to 7	−2 to 6
Validation	0.80–0.86	0.86–0.92	0.85–0.90	0.95–0.95	−7 to 6	10–18

increasing trends over both annual and seasonal time scales (Table 5). In the Kakshaal catchment, trends in simulated annual and seasonal discharge were close to the observed ones. In the Sari-Djaz catchment, the hydrological model showed an underestimation of trends in summer, and an overestimation in autumn. This might be related to a tendency of the GLOFs from Lake Merzbacher occurring earlier in the year, shifting from October to August [*Glazirin*, 2010].

4.2.3. Effect of Changes in Glacier Area and Elevation

The effect of changes in glacier surface geometry was estimated by a set of simulations in which glacier area and glacier surface elevation were kept constant (Table 6). These simulations showed that changes in the glacier geometry had little effect on discharge trends in the less glacierized Kakshaal catchment. In the Sari-Djaz catchment, with a glacierization of 21%, however, not considering changes in glacier geometry resulted in higher discharge increases. The simulations indicate that the changes in glacier geometry reduced the streamflow increases in annual discharge by 14–23% compared to the hypothetical situation of no glacier geometry changes (uncertainty range based on parameter uncertainties; Table 6). Changes in glacier area, which led to lower discharge increases, outweighed the changes in glacier surface elevation, which led to additional increases in discharge. Overall, glacier changes therefore resulted in lower discharge increases as compared to the hypothetical situation of unchanged glacier geometries.

4.2.4. Influence of Temperature and Precipitation Changes on Discharge Trends

The direct effects of the precipitation and temperature changes on the streamflow trends were estimated using simulations with detrended climate time series and a constant glacier geometry. The simulations with detrended time series for both precipitation and temperature resulted in negligible streamflow trends (Table 7). This corroborates that the discharge trends for the model with the original precipitation/temperature data can largely be explained by the changes in these forcing data. Both increases in temperature and precipitation contributed to the discharge increases in the Kakshaal catchment, with a higher influence of the precipitation increases (Table 7). In the Sari-Djaz catchment, changes in precipitation had only very small effects and increases in discharge were mainly caused by the increases in temperature (Table 7).

The overall effect of the temperature and precipitation changes (including glacier geometry changes) can be summarized as follows. For the Kakshaal catchment, it can directly be derived from the simulations with detrended climate input and a constant glacier geometry since glacier geometry changes had hardly any effect on the streamflow trends. The precipitation (temperature) contribution to the streamflow trend may be estimated from the difference between the simulation with original climate input time series and the simulation with the detrended precipitation (temperature) and the original temperature (precipitation) input (Figure 9). Since for the Sari-Djaz catchment, direct effects of temperature and precipitation on streamflow were strongly dominated by temperature, it may tentatively be assumed that the changes in glacier geometry are also largely caused by temperature changes. The overall trend due to temperature changes may thus be estimated from (1) the trend of the simulation considering glacier geometry changes with the original climate input time series, minus (2) the simulation without considering changes in glacier geometry with the detrended temperature and the original precipitation input. The overall trend due to precipitation changes may be estimated from (1) the trend of the simulation with the original climate input time series, minus (2) the simulation with the detrended precipitation and the original temperature input (both without considering changes in glacier geometry) (Figure 9).

We further analyzed changes in simulated contributions of snowmelt, liquid precipitation, and glacier melt to the overall input to the hydrological system (using the model with glacier geometry changes and the

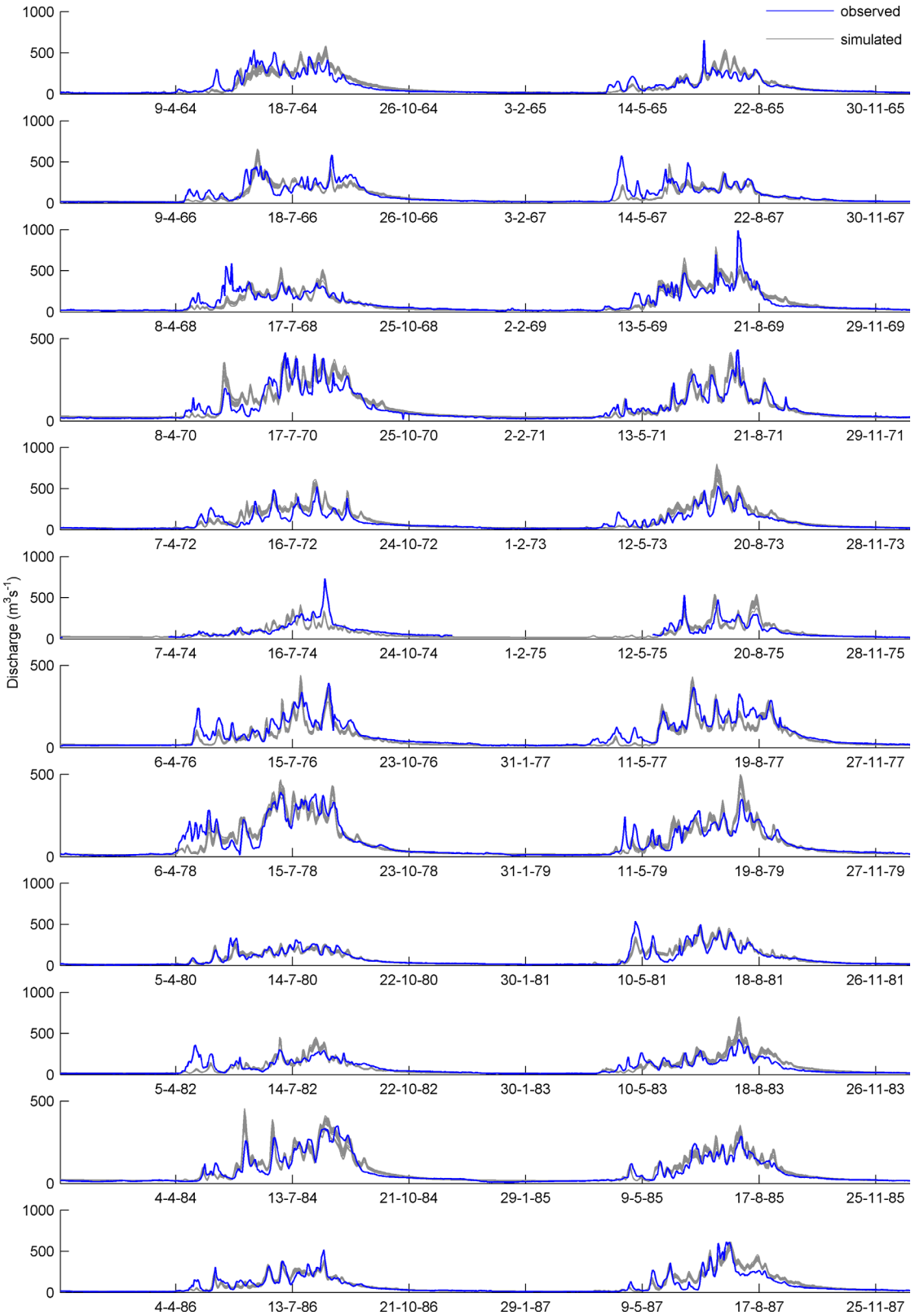

Figure 5. Simulated and observed daily runoff for the period 1964–1987 for the Kakshaal catchment. The simulated discharge includes simulations for all selected parameterizations.

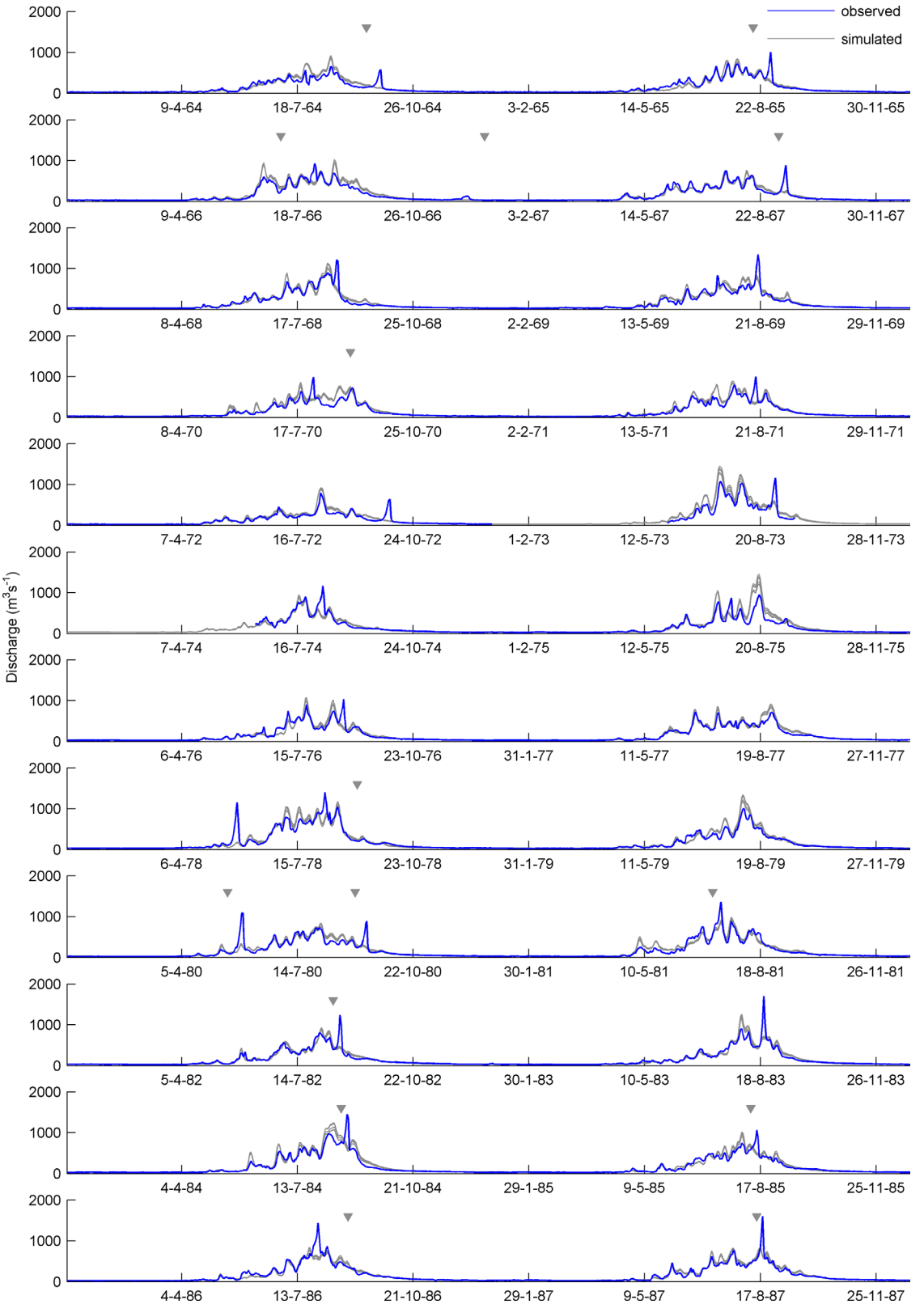

Figure 6. Simulated and observed daily runoff for the period 1964–1987 for the Sari-Djaz catchment. Gray triangles mark the dates of reported GLOFs as listed in *Glazirin* [2010]. The simulated discharge includes simulations for all selected parameterizations.

Table 5. Coefficient of Determination (R^2) Between Annual and Seasonal Simulated (Q_{sim}) and Observed (Q_{obs}) Discharge, As Well As Corresponding Trends Over the Period 1957–2004[a]

		Q_{obs}		Q_{sim}	
	R^2	Trend (mm)	*p*-Value	Trend (mm)	*p*-Value
Kakshaal					
Annual	0.61–0.64	47	<0.01	47–53	<0.01–0.03
Winter	0.57–0.65	3	<0.01	2–3	<0.01–0.02
Spring	0.27–0.29	14	<0.01	9–12	<0.01
Summer	0.62–0.65	27	<0.01	22–27	0.04–0.09
Autumn	0.45–0.62	6	0.02	7–9	<0.01–0.05
Sari-Djaz					
Annual	0.43–0.49	102	<0.01	89–101	<0.01–0.01
Winter	0.19–0.22	3	0.01	1–1	0.03–0.09
Spring	0.10–0.12	7	0.01	8–10	0.01–0.02
Summer	0.41–0.47	74	<0.01	50–57	0.02–0.03
Autumn	0.34–0.36	12	0.10	25–30	<0.01–0.01

[a]For model performance and trends of simulated discharge, the table gives ranges over the selected model parameterizations.

original temperature and precipitation input). This is slightly different from the contributions to discharge, which would be reduced by evapotranspiration and shifted in time by storage delays. In both catchments, the model shows significant increases of glacier melt ($p < 0.01$) and insignificant increases in rainfall and snowmelt ($p > 0.1$) (Table 8 and Figure 10). In the Kakshaal catchment, the model indicates that 13–29% of the changes in water input were due to increased glacier melt, and 71–87% due to increased precipitation, while for the Sari-Djaz catchment, increased glacier melt accounted for 56–85% of the changes in water input and changes in precipitation for 15–44%.

5. Discussion

5.1. Glacier Melt Contribution and Trend Attribution for Two Headwater Catchments of the Aksu River

Our estimates of the glacier melt contribution to runoff of 9–24% for the Kakshaal and 35–48% for the Sari-Djaz are similar to those of *Zhao et al*. [2013], who derived glacier melt contributions of 23 and 44% for the Kakshaal and Sari-Djaz, respectively. *Dikikh* [1993] estimated glacier melt contributions of 24% for the Kakshaal, and 33% for the Sari-Djaz Basin (the latter is called Aksu in their study; glacier contributions calculated from the values for ice melt and total runoff in Table 7 of their study). Including rainfall, snowmelt, and glacier melt from the glacier area, *Aizen and Aizen* [1998] estimated that the glacier areas contributed 36–38% to the total runoff in the Sari-Djaz Basin (called Aksu in their study).

Our results shed new light on the attribution of streamflow trends for the Aksu headwater catchments. Previous studies also indicated that the increase of annual runoff of these two catchments was caused by increases in temperature and precipitation, based on correlations between runoff time series of the Kakshaal and Sari-Djaz catchments with precipitation and temperature time series of meteorological stations [*Xu et al*., 2010; *Zhang et al*., 2010], but did not quantify the role of precipitation or temperature increases. Based on a hydrological simulation approach, a study by *Zhao et al*. [2013] found that discharge increases over the period 1970–2007 were (a) due to precipitation increases alone in the Kakshaal catchment and (b) by 96% due to increases in precipitation and 4% due to increases in glacier melt in the Sari-Djaz catchment.

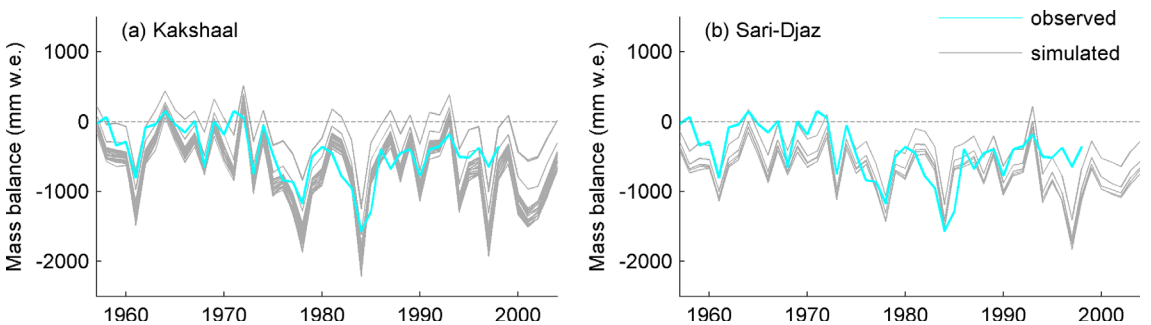

Figure 7. Interannual variation of the observed glacier mass balance at Karabatkak Glacier and of the simulated catchment-average glacier mass balance for (a) the Kakshaal and (b) the Sari-Djaz catchment. The simulated mass balance is represented by all selected parameterizations.

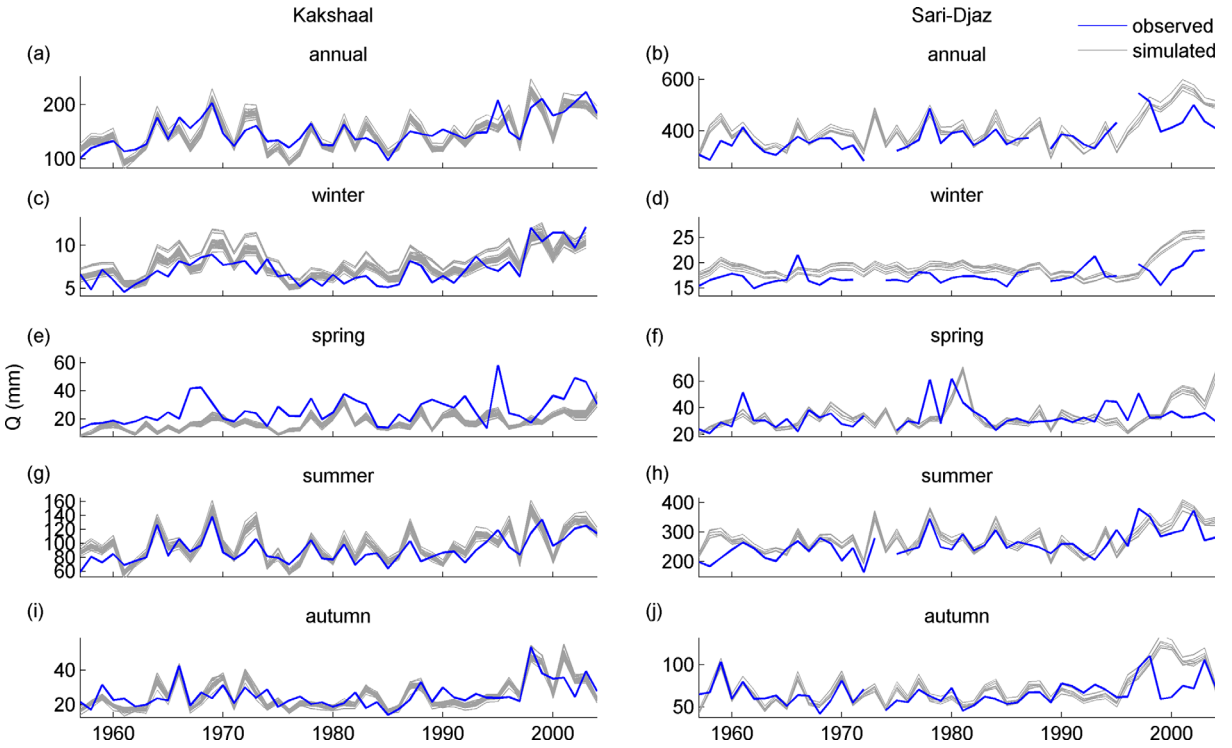

Figure 8. Observed and simulated (a, b) annual and (c–j) seasonal discharge for the Kakshaal and the Sari-Djaz catchment. The simulated discharge includes simulations for all selected parameterizations.

In contrast, our study indicates that precipitation and temperature played both a role for the discharge increases in the Kakshaal catchment, and that temperature increases were the dominant driver in the Sari-Djaz catchment. While the analyzed time periods do not completely overlap, important differences of the current study in comparison to *Zhao et al*. [2013], which may explain these differences, are (1) the additional use of calibration criteria based on glacier mass balance, (2) the attention paid to data consistency during temperature and precipitation interpolation, (3) the representation of glacier geometry changes, (4) the model evaluations for interannual variations in discharge and representation of observed discharge trends, and (5) the consideration of uncertainties resulting from different model parameterizations.

In glacierized catchments, temperature increases are expected to lead to higher glacier melt in an initial phase, later followed by a reduction in glacier melt due to reduced glacier areas. For the catchments in the present study, regression residuals did not show trends over time, indicating that, over the studied period, the catchments may be assumed to be still in the initial phase of increasing discharge. In this phase, the effect of temperature increases on higher melt rates and increases in the ablation area towards higher elevations dominate over the effect of glacier area decreases.

5.2. Data-Based Versus Simulation-Based Trend Attribution

The performance of the regression and simulation models with respect to R^2 and deviation of trends between simulated and observed flows was comparable (Tables 3 and 5). For the high flow season in summer, for example, the simulation model outperformed the regression model in the Kakshaal catchment, while the regression approach showed a higher performance in the Sari-Djaz catchment.

Data-based approaches are typically relatively fast to apply and less affected by model structural and parameter uncertainties. However, it is not always obvious whether the identified statistical relationships are due to physical cause-effect relationships. In the simulation-based approach, changes in streamflow are linked to changes in the drivers via process-based relationships implemented in the model. Furthermore, other data, such as the glacier mass balance data in this study, can be integrated within the modeling approach so that it may also be investigated whether the assumed causes for the changes are consistent

Table 6. Trends Over the Period 1957–2004 and *p*-Values of the Mann-Kendall Test for Time Series of Annual and Seasonal Discharge, As Simulated by the WASA Model With and Without Considering Changes in Glacier Area and Elevation (Ranges Over the Selected Model Parameterizations)[a]

	Change in Glacier Area and Surface Elevation		Constant Glacier Geometry	
	Trend (mm)	*p*-Value	Trend (mm)	*p*-Value
Kakshaal				
Annual	47–53	<0.01–0.03	47–54	<0.01–0.02
Winter	2–3	<0.01–0.02	2–3	<0.01–0.01
Spring	9–12	<0.01	9–12	<0.01
Summer	22–27	0.04–0.09	23–28	0.04–0.09
Autumn	7–9	<0.01–0.05	8–10	<0.01–0.03
Sari-Djaz				
Annual	89–101	<0.01–0.01	105–116	<0.01
Winter	1–1	0.03–0.09	1–1	0.01–0.02
Spring	8–10	0.01–0.02	8–10	0.01–0.02
Summer	50–57	0.02–0.03	60–71	0.01–0.01
Autumn	25–30	<0.01–0.01	29–33	<0.01

[a]The simulations were performed with the original precipitation and temperature time series.

with these data. Disadvantages of the simulation-based approach are the introduction of model parameter and structural uncertainties and the greater effort for setting up the model. This study applied both, a simulation-based and a regression-based approach. The results from the two different approaches correspond well with each other. Since the two methods can be seen as independent, this increases the confidence in the results.

5.3. Multiobjective Model Calibration

Including objective functions on different variables can highlight discrepancies between the model and the different data sets, which can give directions where further research should focus. The trade-off between the model performance with respect to discharge and the glacier mass balance time series in the Sari-Djaz Basin indicates possible problems in the model or the data. The reason is currently unclear. The temporal dynamics of Karabatkak Glacier may not be representative for the temporal dynamics of a larger number of glaciers, even though typically temporal mass balance variations are assumed to correlate well at the scale of mountain ranges [*Huss*, 2012]. Other possible causes are errors in the measured mass balance time series (which could be related to the difficulty to access the accumulation area of Karabatkak Glacier), errors in other model calibration or input data, or model structural errors. A new study indicates geodetic glacier mass balance estimates of -0.35 ± 0.34 m w.e. a^{-1} for the time period 1974–1999 for the Sari-Djaz Basin [*Pieczonka and Bolch*, 2015], which largely overlaps with the glacier mass balance criterion applied in this study. Geodetic mass balance estimates derived specifically for the Kakshaal catchment could reduce the uncertainties resulting from the use of mass balance estimates of neighboring regions.

Evaluating the model behavior with respect to the observed variability in the past is also a good model test if it is intended to apply the model to estimate streamflow changes in response to climate scenarios. This could for example reveal problems of the model related to instabilities of the model parameters over time [*Merz et al.*, 2011]. Studies which apply a hydrological model for climate change scenarios often evaluate

Table 7. Trends Over the Period 1957–2004 and *p*-Values of the Mann-Kendall Test for Simulated Time Series of Annual and Seasonal Discharge, As Ranges Over the Selected Model Parameterizations[a]

	Original P, Original T		Detrended P, Detrended T		Original P, Detrended T		Detrended P, Original T	
	Trend (mm)	*p*-Value	Trend (mm)	*p*-Value	Trend (mm)	*p*-Value	Trend (mm)	*p*-Value
Kakshaal								
Annual	47–54	<0.01–0.02	0–3	0.04–0.78	35–45	0.07–0.12	11–22	0.01–0.05
Winter	2–3	<0.01–0.01	0–0	<0.01–0.31	2–3	<0.01–0.02	0–1	<0.01–0.09
Spring	9–12	<0.01	0–0	0.27–0.88	7–10	<0.01	6–7	0.01–0.03
Summer	23–28	0.04–0.09	0–2	0.08–0.91	15–23	0.25–0.40	1–7	0.22–0.65
Autumn	8–10	<0.01–0.03	0–1	0.01–0.32	4–7	0.08–0.15	3–6	0.01–0.17
Sari-Djaz								
Annual	105–116	<0.01	3–6	0.17–0.59	2–6	0.81–0.92	92–107	<0.01
Winter	1–1	0.01–0.02	0–1	<0.01–0.02	−1 to −1	0.17–0.22	4–4	<0.01
Spring	8–10	0.01–0.02	0–0	0.32–0.53	1–2	0.70–0.95	10–11	<0.01–0.01
Summer	60–71	0.01–0.01	1–3	0.12–0.45	2–3	0.87–0.99	50–59	0.01–0.01
Autumn	29–33	<0.01	1–2	0.38–0.49	−4 to −3	0.33–0.38	27–31	<0.01

[a]The simulations were performed with different combinations of original and detrended precipitation and temperature time series, keeping the glacier geometry constant.

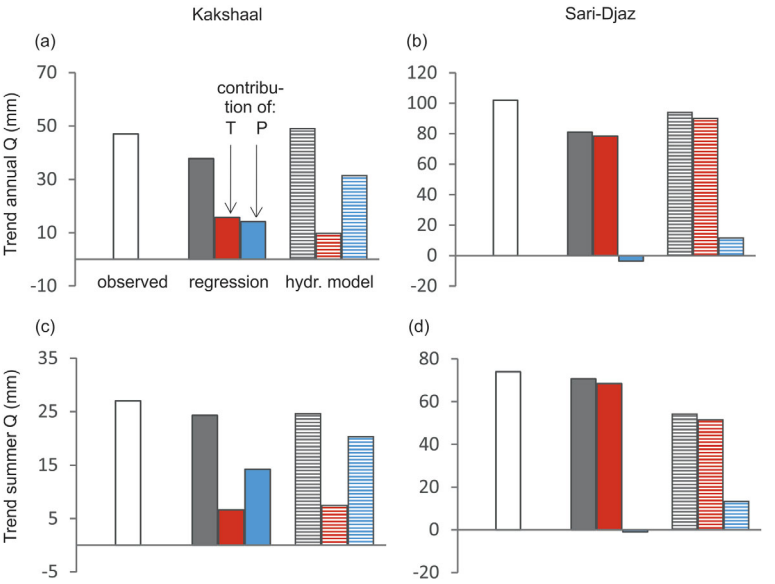

Figure 9. Contributions of precipitation and temperature to the annual and summer streamflow trends in the Kakshaal and the Sari-Djaz catchment as estimated with the regression model (filled bars) and with the hydrological model (striped bars). White: observed trend, gray: modeled trend with original input, red: temperature contribution to trend, and blue: precipitation contribution to trend.

the model performance only by using classical criteria like the Nash-Sutcliffe criterion on a daily or monthly time scale [e.g., *Liu et al*., 2010]. As mountain catchments often have a strong seasonal regime, this results in apparently high model performance for all models which can replicate this behavior [*Schaefli and Gupta*, 2007]. However, if a model is planned to be applied for climate change scenarios, it is crucial that also the performance with respect to interannual variability and possible long-term trends is included as this is the critical part of the model with respect to scenario analyses.

Satellite-derived snow cover data can be a further data source for multiobjective model calibration in snow-dominated, data sparse regions [*Duethmann et al*., 2014]. Our analysis of MODIS snow cover data for the study region showed only few, short-lasting snowfall events during the winter season. In this region, winter precipitation is low, and the thin snow cover may be redistributed by wind or removed by sublimation. Since these processes are not represented in the model, using the satellite-derived snow cover data for model calibration with the model in its current form would result in compensating effects (e.g., model parameters might be drawn toward allowing melt at very low temperatures), thus increasing errors in the internal functioning of the model. This highlights the need for careful data analysis before their application for model calibration. Due to the very low amounts of winter precipitation, we assume that neglecting the processes of sublimation and snow redistribution before melt onset has only small effects on the overall performance of the hydrological model.

Table 8. Trends Over the Period 1957–2004 in the Simulated Inputs to the Hydrological System by Rain, Snowmelt, and Glacier Melt Over the 48 Year Study Period for the Two Study Catchments, Calculated With the Sen's Slope Estimator and the Mann-Kendall Test

	Trend (mm)	*p*-Value of Trend	Contribution to Overall Trend in Simulated Water Input (%)
Kakshaal			
Rain	35–42	0.13–0.25	42–59
Snowmelt	16–24	0.26–0.46	22–30
Glacier melt	9–24	<0.01–0.01	13–29
Sari-Djaz			
Rain	12–15	0.82–0.91	14–17
Snowmelt	−1 to 24	0.41–0.99	−1 to 27
Glacier melt	49–73	<0.01–0.01	56–85

5.4. Limitations

The temporal variability of temperature and precipitation was derived from the available data and may not be representative for all subregions. It was not clear whether precipitation data of the station Tien Shan, which were left in the analysis, are not influenced by the relocation. Based on our analyses performed without including the station Tien Shan, it is assumed that omitting this station from

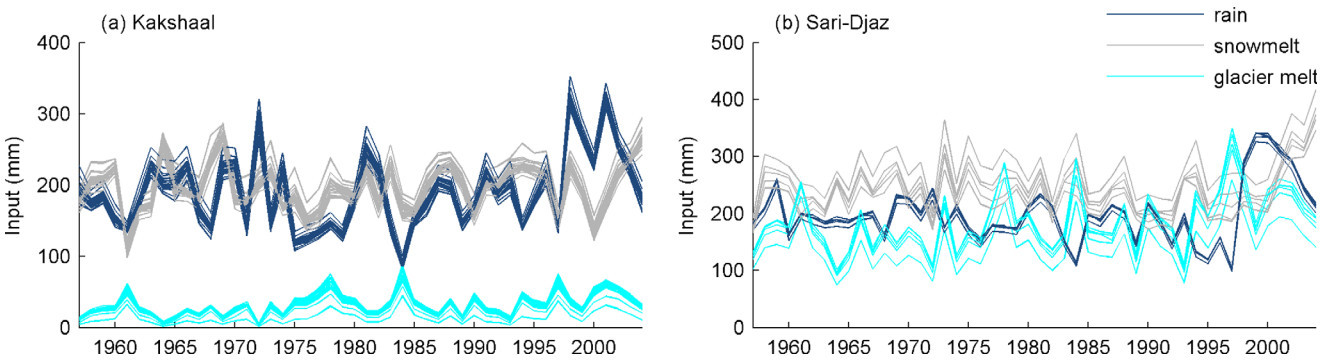

Figure 10. Annual variation of the input from snowmelt, glacier melt, and rain, as represented in the WASA model for the selected model parameterizations for (a) the Kakshaal and (b) the Sari-Djaz catchment.

the interpolation of precipitation data would mainly influence results of the Sari-Djaz catchment. The analysis would likely attribute a larger part of the discharge increases also to increases in precipitation, but temperature increases would probably still play the dominant role for increases in discharge.

The initial glacier elevation in the hydrological model was based on the SRTM DEM, as a DEM for the entire study area at the beginning of the study period was not available. Absolute glacier elevations are therefore underestimated. This is partly compensated by the calibrated parameters and is assumed to have little effect on the estimated trends in glacier melt and discharge. It is to note that the lowering of the glacier surface elevation during the study period, which has an influence on the trends, is represented in the model.

This study considered direct effects of meteorological drivers on evapotranspiration. In contrast, indirect effects through possible changes in vegetation and in the length of the growing period were not accounted for. Thus, the increase in evapotranspiration may have been underestimated. Due to the generally low temperatures at high altitudes, this effect is, however, assumed not to be very large.

While our approach accounted for uncertainties in model parameters, uncertainties from different model structures were not considered. These could be explored using an ensemble of hydrological models.

6. Conclusions

This study used two approaches based on regression analysis and hydrological modeling to understand the recent increase in discharge in two headwater catchments of the Tarim River. For the more strongly glacierized Sari-Djaz catchment, both approaches agree on the dominant role of increasing temperatures as cause for the discharge changes. Simulated changes in the input contributions from rain, snowmelt, and glacier melt show that increases in the overall input to the hydrological system were dominated by increases in glacier melt, which contributed 56–85% to the overall increases in water input. In the Kakshaal catchment, increasing discharge over the last decades was related to both increasing temperatures and increasing precipitation. The hydrological model showed that increases in glacier melt in the Kakshaal catchment contributed 13–29% to the overall increases in water input from rain, snowmelt, and glacier melt, while the major part of the increases to the water input was from increased precipitation.

The simulations indicated glacier melt contributions to runoff of 9–24% for the Kakshaal, and 35–48% for the Sari-Djaz catchment. The analysis highlighted large uncertainties of areal precipitation in data-sparse mountain regions of Central Asia. With values of about 370–400 mm a^{-1} for the Kakshaal and 450–530 mm a^{-1} for the Sari-Djaz catchment, the areal precipitation estimates adjusted by model calibration indicated that the original estimates based on interpolation of station data underestimated by about 50%.

Using calibration criteria based on glacier mass balances and the interannual variation of discharge in addition to the performance with respect to daily discharge led to more credible models. This is particularly important in such data-sparse catchments. In strongly seasonal discharge regimes, high performance with respect to monthly or daily streamflow can result in overestimation of the skill of the model. An evaluation with respect to the interannual variability of, e.g., seasonal flow can be a good measure to indicate whether

the model responds adequately to interannual changes in temperature and precipitation, which is a prerequisite for models set up for climate change impact analyses.

While data-based approaches for trend attribution are simpler to implement and thus particularly suited to give insights for a large number of catchments, simulation-based approaches have the advantage that the cause-effect relationships can be represented in a process-based way, which suggests that their results can provide stronger evidence for trend attribution. Where possible, a complementary application of both approaches is recommended.

Acknowledgments
Simulation data of this study can be obtained from the first author (doris.duethmann@gfz-potsdam.de). This study was conducted within the project SuMaRiO (Sustainable Management of River Oases along the Tarim River; http://www.sumario.de/), funded by the German Federal Ministry of Education and Research (BMBF grants 01LL0918A and 01LL0918B). T. Bolch and D. Farinotti were supported by the German Research Foundation (DFG, Code BO 3199/2-1) and the Swiss National Science Foundation, respectively. We thank Vladimir Aizen for providing the digital elevation models for the Ak-Shirak massif and the Hydrometeorological Service of Kyrgyzstan for providing meteorological data. We are grateful to two anonymous reviewers, Ludwig Braun, and the Associate Editor for their constructive comments.

References

Aguado, E., D. Cayan, L. Riddle, and M. Roos (1992), Climatic fluctuations and the timing of West Coast streamflow, *J. Clim.*, *5*(12), 1468–1483.

Aizen, V. B., and E. M. Aizen (1998), Estimation of glacial runoff to the Tarim River, Central Tien Shan, in *Hydrology, Water Resources and Ecology in Headwaters*, vol. 248, pp. 191–198, IAHS Publ., Meran, Italy.

Aizen, V. B., E. M. Aizen, and J. M. Melack (1995), Climate, snow cover, glaciers, and runoff in the Tien-Shan, Central-Asia, *Water Resour. Bull.*, *31*(6), 1113–1129.

Aizen, V. B., E. M. Aizen, J. Dozier, J. M. Melack, D. D. Sexton, and V. N. Nesterov (1997), Glacial regime of the highest Tien Shan mountain, Pobeda-Khan Tengry massif, *J. Glaciol.*, *43*(145), 503–512.

Aizen, V. B., V. A. Kuzmichenok, A. B. Surazakov, and E. M. Aizen (2006), Glacier changes in the central and northern Tien Shan during the last 140 years based on surface and remote-sensing data, *Ann. Glaciol.*, *43*(1), 202–213.

Anderson, E. A. (1973), National Weather Service river forecast system—Snow accumulation and ablation model, *NOAA Tech. Memo. NWS-HYDRO-17*, 217 pp., U.S. Dep. of Commer., NOAA, NWS, Washington, D. C.

Baraer, M., B. G. Mark, J. M. McKenzie, T. Condom, J. Bury, K.-I. Huh, C. Portocarrero, J. Gomez, and S. Rathay (2012), Glacier recession and water resources in Peru's Cordillera Blanca, *J. Glaciol.*, *58*(207), 134–150.

Barnett, T. P., J. C. Adam, and D. P. Lettenmaier (2005), Potential impacts of a warming climate on water availability in snow-dominated regions, *Nature*, *438*(7066), 303–309.

Bengtsson, L., K. I. Hodges, and S. Hagemann (2004), Sensitivity of the ERA-40 reanalysis to the observing system: Determination of the global atmospheric circulation from reduced observations, *Tellus, Ser. A*, *56*(5), 456–471.

Birsan, M.-V., P. Molnar, P. Burlando, and M. Pfaundler (2005), Streamflow trends in Switzerland, *J. Hydrol.*, *314*(1), 312–329.

Bothe, O., K. Fraedrich, and X. H. Zhu (2012), Precipitation climate of Central Asia and the large-scale atmospheric circulation, *Theor. Appl. Climatol.*, *108*(3–4), 345–354.

Chen, M. Y., P. P. Xie, J. E. Janowiak, and P. A. Arkin (2002), Global land precipitation: A 50-yr monthly analysis based on gauge observations, *J. Hydrometeorol.*, *3*(3), 249–266.

Chen, Y., C. Xu, X. Hao, W. Li, Y. Chen, C. Zhu, and Z. Ye (2009), Fifty-year climate change and its effect on annual runoff in the Tarim River Basin, China, *Quat. Int.*, *208*(1), 53–61.

Collins, D. N. (1987), Climatic fluctuations and runoff from glacierised Alpine basins, in *The Influence of Climate Change and Climatic Variability on the Hydrologic Regime and Water Resources*, vol. 168, pp. 77–89, IAHS Publ., Vancouver, B. C., Canada.

Dahlke, H. E., S. W. Lyon, J. Stedinger, G. Rosqvist, P. Jansson, and M. Weiler (2012), Contrasting trends in floods for two sub-arctic catchments in northern Sweden—Does glacier presence matter?, *Hydrol. Earth Syst. Sci.*, *16*(7), 2123–2141.

Daly, C. (2006), Guidelines for assessing the suitability of spatial climate data sets, *Int. J. Climatol.*, *26*(6), 707–721.

Dee, D. P., et al. (2011), The ERA-Interim reanalysis: Configuration and performance of the data assimilation system, *Q. J. R. Meteorol. Soc.*, *137*(656), 553–597.

Dery, S. J., K. Stahl, R. D. Moore, P. H. Whitfield, B. Menounos, and J. E. Burford (2009), Detection of runoff timing changes in pluvial, nival, and glacial rivers of western Canada, *Water Resour. Res.*, *45*, W06701, doi:10.1029/2008WR006975.

Dettinger, M. D., and D. R. Cayan (1995), Large-scale atmospheric forcing of recent trends toward early snowmelt runoff in California, *J. Clim.*, *8*(3), 606–623.

Dikikh, A. (1993), Lednikoviy stok rek Tyan-Shanya i ego rol' v formirovanii obshego stoka [Glacier runoff in the rivers of Tien Shan and its role in total runoff formation], *Mater. Glaciol. Issled.*, *77*, 41–50.

Draper, N. R., and H. Smith (1998), *Applied Regression Analysis*, 3rd ed., John Wiley, N. Y.

Duethmann, D., J. Zimmer, A. Gafurov, A. Güntner, D. Kriegel, B. Merz, and S. Vorogushyn (2013), Evaluation of areal precipitation estimates based on downscaled reanalysis and station data by hydrological modelling, *Hydrol. Earth Syst. Sci.*, *17*(7), 2415–2434.

Duethmann, D., J. Peters, T. Blume, S. Vorogushyn, and A. Güntner (2014), The value of satellite-derived snow cover images for calibrating a hydrological model in snow-dominated catchments in Central Asia, *Water Resour. Res.*, *50*, 2002–2021, doi:10.1002/2013WR014382.

Dyurgerov, M. B., and M. F. Meier (2005), Glaciers and the changing earth system: A 2004 snapshot, *Occas. Pap. 58*, 117 pp., Inst. of Arct. and Alp. Res., Univ. of Colo. Boulder, Boulder, Colo.

Engelhardt, M., T. V. Schuler, and L. M. Andreassen (2014), Contribution of snow and glacier melt to discharge for highly glacierised catchments in Norway, *Hydrol. Earth Syst. Sci.*, *18*(2), 511–523.

Fan, Y. T., Y. N. Chen, W. H. Li, H. J. Wang, and X. G. Li (2011), Impacts of temperature and precipitation on runoff in the Tarim River during the past 50 years, *J. Arid Land*, *3*(3), 220–230.

FAO/IIASA/ISRIC/ISS-CAS/JRC (2012), *Harmonized World Soil Database*, *Version 1.2*, FAO, Rome. [Available at http://www.iiasa.ac.at/Research/LUC/External-World-soil-database/HTML/.]

Farinotti, D., S. Usselmann, M. Huss, A. Bauder, and M. Funk (2012), Runoff evolution in the Swiss Alps: Projections for selected high-alpine catchments based on ENSEMBLES scenarios, *Hydrol. Processes*, *26*(13), 1909–1924.

Feng, Q., K. N. Endo, and G. D. Cheng (2001), Towards sustainable development of the environmentally degraded arid rivers of China—A case study from Tarim River, *Environ. Geol.*, *41*(1–2), 229–238.

Fleming, S. W., and G. K. Clarke (2003), Glacial control of water resource and related environmental responses to climatic warming: Empirical analysis using historical streamflow data from northwestern Canada, *Can. Water Resour. J.*, *28*(1), 69–86.

Francke, T., A. Güntner, G. Mamede, E. N. Müller, and A. Bronstert (2008), Automated catena-based discretization of landscapes for the derivation of hydrological modelling units, *Int. J. Geogr. Inf. Sci.*, *22*(2), 111–132.

Frey, H., H. Machguth, M. Huss, C. Huggel, S. Bajracharya, T. Bolch, A. Kulkarni, A. Linsbauer, N. Salzmann, and M. Stoffel (2014), Estimating the volume of glaciers in the Himalayan-Karakoram region using different methods, *Cryosphere*, *8*(6), 2313–2333.
Friedl, M. A., et al. (2002), Global land cover mapping from MODIS: Algorithms and early results, *Remote Sens. Environ.*, *83*(1–2), 287–302.
Glazirin, G. E. (2010), A century of investigations on outbursts of the ice-dammed Lake Merzbacher (Central Tien Shan), *Aust. J. Earth Sci.*, *103*(2), 171–179.
Güntner, A. (2002), Large-scale hydrological modelling in the semi-arid North-East of Brazil, *PIK Rep. 77*, 128 pp., Potsdam Inst. for Clim. Impact Res., Potsdam, Germany.
Güntner, A., and A. Bronstert (2004), Representation of landscape variability and lateral redistribution processes for large-scale hydrological modelling in semi-arid areas, *J. Hydrol.*, *297*(1–4), 136–161.
Hamlet, A. F., P. W. Mote, M. P. Clark, and D. P. Lettenmaier (2005), Effects of temperature and precipitation variability on snowpack trends in the western United States, *J. Clim.*, *18*(21), 4545–4561.
Hamlet, A. F., P. W. Mote, M. P. Clark, and D. P. Lettenmaier (2007), Twentieth-century trends in runoff, evapotranspiration, and soil moisture in the western United States, *J. Clim.*, *20*(8), 1468–1486.
Hidalgo, H. G., et al. (2009), Detection and attribution of streamflow timing changes to climate change in the western United States, *J. Clim.*, *22*(13), 3838–3855.
Hock, R. (2003), Temperature index melt modelling in mountain areas, *J. Hydrol.*, *282*(1–4), 104–115.
Huss, M. (2012), Extrapolating glacier mass balance to the mountain-range scale: The European Alps 1900–2100, *Cryosphere*, *6*(4), 713–727.
Huss, M., G. Jouvet, D. Farinotti, and A. Bauder (2010), Future high-mountain hydrology: A new parameterization of glacier retreat, *Hydrol. Earth Syst. Sci.*, *14*(5), 815–829.
Huss, M., R. Hock, A. Bauder, and M. Funk (2012), Conventional versus reference-surface mass balance, *J. Glaciol.*, *58*(208), 278–286.
Immerzeel, W. W., N. Wanders, A. F. Lutz, J. M. Shea, and M. F. P. Bierkens (2015), Reconciling high altitude precipitation in the upper Indus Basin with glacier mass balances and runoff, *Hydrol. Earth Syst. Sci. Discuss.*, *12*(5), 4755–4784.
Jansson, P., R. Hock, and T. Schneider (2003), The concept of glacier storage: A review, *J. Hydrol.*, *282*(1–4), 116–129.
Jarvis, A., H. I. Reuter, A. Nelson, and E. Guevara (2008), *Holefilled Seamless SRTM Data*, Int. Cent. for Trop. Agric., Calif., Colombia. [Available at http://srtm.csi.cgiar.org.]
Jinshi, L. (1992), Jökulhlaups in the Kunmalike River, southern Tien Shan mountains, China, *Ann. Glaciol.*, *16*, 85–88.
Jost, G., R. D. Moore, B. Menounos, and R. Wheate (2012), Quantifying the contribution of glacier runoff to streamflow in the upper Columbia River Basin, Canada, *Hydrol. Earth Syst. Sci.*, *16*(3), 849–860.
Kendall, M. G. (1975), *Rank Correlation Methods*, 4th ed., 196 pp., Charles Griffin, London, U. K.
Kollat, J. B., and P. M. Reed (2006), Comparing state-of-the-art evolutionary multi-objective algorithms for long-term groundwater monitoring design, *Adv. Water Resour.*, *29*(6), 792–807.
Konz, M., and J. Seibert (2010), On the value of glacier mass balances for hydrological model calibration, *J. Hydrol.*, *385*(1–4), 238–246.
Kormann, C., T. Francke, M. Renner, and A. Bronstert (2015), Attribution of high resolution streamflow trends in Western Austria—An approach based on climate and discharge station data, *Hydrol. Earth Syst. Sci.*, *19*(3), 1225–1245.
Kriegel, D., C. Mayer, W. Hagg, S. Vorogushyn, D. Duethmann, A. Gafurov, and D. Farinotti (2013), Changes in glacierisation, climate and runoff in the second half of the 20th century in the Naryn Basin, Central Asia, *Global Planet. Change*, *110*, 51–61.
Krysanova, V., M. Wortmann, T. Bolch, B. Merz, D. Duethmann, J. Walter, S. Huang, T. Jiang, B. Su, and Z. Kundzewicz (2014), Analysis of current trends in climate parameters, river discharge and glaciers in the Aksu River basin (Central Asia), *Hydrol. Sci. J.*, *60*(4), 566–590.
Kundzewicz, Z., B. Merz, S. Vorogushyn, H. Hartmann, D. Duethmann, M. Wortmann, S. Huang, B. Su, T. Jiang, and V. Krysanova (2015), Analysis of changes in climate and river discharge with focus on seasonal runoff predictability in the Aksu River Basin, *Environ. Earth Sci.*, *73*(2), 501–516.
Leiwen, J., T. Yufen, Z. Zhijie, L. Tianhong, and L. Jianhua (2005), Water resources, land exploration and population dynamics in arid areas-the case of the Tarim River basin in Xinjiang of China, *Popul. Environ.*, *26*(6), 471–503.
Li, Z., W. Wang, M. Zhang, F. Wang, and H. Li (2010), Observed changes in streamflow at the headwaters of the Urumqi River, eastern Tianshan, central Asia, *Hydrol. Processes*, *24*(2), 217–224.
Lilliefors, H. W. (1967), On the Kolmogorov-Smirnov test for normality with mean and variance unknown, *J. Am. Stat. Assoc.*, *62*(318), 399–402.
Linsbauer, A., F. Paul, and W. Haeberli (2012), Modeling glacier thickness distribution and bed topography over entire mountain ranges with GlabTop: Application of a fast and robust approach, *J. Geophys. Res.*, *117*, F03007, doi:10.1029/2011JF002313.
Liston, G. E. (2004), Representing subgrid snow cover heterogeneities in regional and global models, *J. Clim.*, *17*(6), 1381–1397.
Liu, S., Y. Ding, D. Shangguan, Y. Zhang, J. Li, H. Han, J. Wang, and C. Xie (2006), Glacier retreat as a result of climate warming and increased precipitation in the Tarim river basin, northwest China, *Ann. Glaciol.*, *43*(1), 91–96.
Liu, Z. F., Z. X. Xu, J. X. Huang, S. P. Charles, and G. B. Fu (2010), Impacts of climate change on hydrological processes in the headwater catchment of the Tarim River basin, China, *Hydrol. Processes*, *24*(2), 196–208.
Ljung, G. M., and G. E. Box (1978), On a measure of lack of fit in time series models, *Biometrika*, *65*(2), 297–303.
Mann, H. (1945), Non-parametric test against trend, *Econometrica*, *13*, 245–259.
Mayr, E., W. Hagg, C. Mayer, and L. Braun (2013), Calibrating a spatially distributed conceptual hydrological model using runoff, annual mass balance and winter mass balance, *J. Hydrol.*, *478*, 40–49.
Merz, B., S. Vorogushyn, S. Uhlemann, J. Delgado, and Y. Hundecha (2012), More efforts and scientific rigour are needed to attribute trends in flood time series, *Hydrol. Earth Syst. Sci.*, *16*(5), 1379–1387.
Merz, R., J. Parajka, and G. Blöschl (2011), Time stability of catchment model parameters: Implications for climate impact analyses, *Water Resour. Res.*, *47*, W02531, doi:10.1029/2010WR009505.
Molnar, P., P. Burlando, and F. Pellicciotti (2011), Streamflow trends in mountainous regions, in *Encyclopedia of Snow, Ice and Glaciers*, edited by V. P. Singh and U. K. Haritashya, pp. 1084–1089, Springer, Dordrecht, Netherlands.
Moore, R., and M. Demuth (2001), Mass balance and streamflow variability at Place Glacier, Canada, in relation to recent climate fluctuations, *Hydrol. Processes*, *15*(18), 3473–3486.
Moore, R. D., S. W. Fleming, B. Menounos, R. Wheate, A. Fountain, K. Stahl, K. Holm, and M. Jakob (2009), Glacier change in western North America: Influences on hydrology, geomorphic hazards and water quality, *Hydrol. Processes*, *23*(1), 42–61.
Mote, P. W. (2006), Climate-driven variability and trends in mountain snowpack in western North America, *J. Clim.*, *19*(23), 6209–6220.
Narama, C., A. Kääb, M. Duishonakunov, and K. Abdrakhmatov (2010), Spatial variability of recent glacier area changes in the Tien Shan Mountains, Central Asia, using Corona (similar to 1970), Landsat (similar to 2000), and ALOS (similar to 2007) satellite data, *Global Planet. Change*, *71*(1–2), 42–54.

Nolin, A. W., J. Phillippe, A. Jefferson, and S. L. Lewis (2010), Present-day and future contributions of glacier runoff to summertime flows in a Pacific Northwest watershed: Implications for water resources, *Water Resour. Res.*, *46*, W12509, doi:10.1029/2009WR008968.
Osmonov, A., T. Bolch, C. Xi, A. Kurban, and W. Guo (2013), Glacier characteristics and changes in the Sary-Jaz River Basin (Central Tien Shan, Kyrgyzstan) 1990–2010, *Remote Sens. Lett.*, *4*(8), 725–734.
Paul, F. (2010), The influence of changes in glacier extent and surface elevation on modeled mass balance, *Cryosphere*, *4*(4), 569–581.
Pellicciotti, F., A. Bauder, and M. Parola (2010), Effect of glaciers on streamflow trends in the Swiss Alps, *Water Resour. Res.*, *46*, W10522, doi: 10.1029/2009WR009039.
Pieczonka, T., and T. Bolch (2015), Region-wide glacier mass budgets and area changes for the Central Tien Shan between ~1975 and 1999 using Hexagon KH-9 imagery, *Global Planet. Change*, *128*, 1–13.
Pieczonka, T., T. Bolch, W. Junfeng, and L. Shiyin (2013), Heterogeneous mass loss of glaciers in the Aksu-Tarim Catchment (Central Tien Shan) revealed by 1976 KH-9 Hexagon and 2009 SPOT-5 stereo imagery, *Remote Sens. Environ.*, *130*, 233–244.
Schaefli, B., and H. V. Gupta (2007), Do Nash values have value?, *Hydrol. Processes*, *21*(15), 2075–2080.
Schaefli, B., and M. Huss (2011), Integrating point glacier mass balance observations into hydrologic model identification, *Hydrol. Earth Syst. Sci.*, *15*(4), 1227–1241.
Schaefli, B., B. Hingray, M. Niggli, and A. Musy (2005), A conceptual glacio-hydrological model for high mountainous catchments, *Hydrol. Earth Syst. Sci.*, *9*(1–2), 95–109.
Schwarz, G. (1978), Estimating the dimension of a model, *Ann. Stat.*, *6*(2), 461–464.
Sen, P. K. (1968), Estimates of the regression coefficient based on Kendall's tau, *J. Am. Stat. Assoc.*, *63*(324), 1379–1389.
Sorg, A., T. Bolch, M. Stoffel, O. Solomina, and M. Beniston (2012), Climate change impacts on glaciers and runoff in Tien Shan (Central Asia), *Nat. Clim. Change*, *2*(10), 725–731.
St Jacques, J.-M., D. J. Sauchyn, and Y. Zhao (2010), Northern Rocky Mountain streamflow records: Global warming trends, human impacts or natural variability?, *Geophys. Res. Lett.*, *37*, L06407, doi:10.1029/2009GL042045.
Stahl, K., and R. D. Moore (2006), Influence of watershed glacier coverage on summer streamflow in British Columbia, Canada, *Water Resour. Res.*, *42*, W06201, doi:10.1029/2006WR005022.
Stahl, K., R. D. Moore, J. M. Shea, D. Hutchinson, and A. J. Cannon (2008), Coupled modelling of glacier and streamflow response to future climate scenarios, *Water Resour. Res.*, *44*, W02422, doi:10.1029/2007WR005956.
Surazakov, A. B., and V. B. Aizen (2006), Estimating volume change of mountain glaciers using SRTM and map-based topographic data, *IEEE Trans. Geosci. Remote Sens.*, *44*(10), 2991–2995.
Tang, Q. H., H. P. Hu, T. K. Oki, and F. Q. Tian (2007), Water balance within intensively cultivated alluvial plain in an arid environment, *Water Resour. Manage.*, *21*(10), 1703–1715.
Tang, Y., P. Reed, and T. Wagener (2006), How effective and efficient are multiobjective evolutionary algorithms at hydrologic model calibration?, *Hydrol. Earth Syst. Sci.*, *10*(2), 289–307.
Tao, H., M. Gemmer, Y. G. Bai, B. D. Su, and W. Y. Mao (2011), Trends of streamflow in the Tarim River Basin during the past 50 years: Human impact or climate change?, *J. Hydrol.*, *400*(1–2), 1–9.
Thevs, N. (2011), Water scarcity and allocation in the Tarim Basin: Decision structures and adaptations on the local level, *J. Curr. Chin. Affairs*, *40*(3), 113–137.
Unger-Shayesteh, K., S. Vorogushyn, D. Farinotti, A. Gafurov, D. Duethmann, A. Mandychev, and B. Merz (2013), What do we know about past changes in the water cycle of Central Asian headwaters? A review, *Global Planet. Change*, *110*, 4–25.
Uppala, S. M., et al. (2005), The ERA-40 re-analysis, *Q. J. R. Meteorol. Soc.*, *131*(612), 2961–3012.
Wang, Y. (2006), *Local Records of the Akesu River Basin*, 719 pp., Fangzi Publ., Beijing.
Weedon, G. P., S. Gomes, P. Viterbo, W. J. Shuttleworth, E. Blyth, H. Osterle, J. C. Adam, N. Bellouin, O. Boucher, and M. Best (2011), Creation of the WATCH forcing data and its use to assess global and regional reference crop evaporation over land during the twentieth century, *J. Hydrometeorol.*, *12*(5), 823–848.
Weedon, G. P., G. Balsamo, N. Bellouin, S. Gomes, M. J. Best, and P. Viterbo (2014), The WFDEI meteorological forcing data set: WATCH forcing data methodology applied to ERA-Interim reanalysis data, *Water Resour. Res.*, *50*, 7505–7514, doi:10.1002/2014WR015638.
WGMS (2012), *Fluctuations of Glaciers 2005–2010*, 366 pp., ICSU(WDS)/IUGG(IACS)/UNEP/UNESCO/WMO, World Glacier Monit. Serv., Zurich, Switzerland.
Wortmann, M., V. Krysanova, Z. Kundzewicz, B. Su, and X. Li (2013), Assessing the influence of the Merzbacher Lake outburst floods on discharge using the hydrological model SWIM in the Aksu headwaters, Kyrgyzstan/NW China, *Hydrol. Processes*, *28*(26), 6337–6350.
Xu, H., B. Zhou, and Y. Song (2010), Impacts of climate change on headstream runoff in the Tarim River Basin, *Hydrol. Res.*, *42*(1), 20–29.
Yue, S., P. Pilon, B. Phinney, and G. Cavadias (2002), The influence of autocorrelation on the ability to detect trend in hydrological series, *Hydrol. Processes*, *16*(9), 1807–1829.
Yue, S., P. Pilon, and B. Phinney (2003), Canadian streamflow trend detection: Impacts of serial and cross-correlation, *Hydrol. Sci. J.*, *48*(1), 51–63.
Zhang, Q., C.-Y. Xu, H. Tao, T. Jiang, and Y. Chen (2010), Climate changes and their impacts on water resources in the arid regions: A case study of the Tarim River basin, China, *Stochastic Environ. Res. Risk Assess.*, *24*(3), 349–358.
Zhao, Q., B. Ye, Y. Ding, S. Zhang, S. Yi, J. Wang, D. Shangguan, C. Zhao, and H. Han (2013), Coupling a glacier melt model to the variable infiltration capacity (VIC) model for hydrological modeling in north-western China, *Environ. Earth Sci.*, *68*(1), 87–101.
Zhou, D., G. Luo, and L. Lu (2010), Processes and trends of the land use change in Aksu watershed in the central Asia from 1960 to 2008, *J. Arid Land*, *2*(3), 157–166.